UNIVERSIDAD DE CONCEPCIÓN

Centro de Investigación en Ingeniería Matemática (CI^{2}MA)

A posteriori error analysis of an augmented fully-mixed formulation for the stationary Boussinesq model

Eligio Colmenares, Gabriel N. Gatica,
Ricardo Oyarzúa

PREPRINT 2017-17

SERIE DE PRE-PUBLICACIONES

A posteriori error analysis of an augmented fully–mixed formulation for the stationary Boussinesq model*

Eligio Colmenares† Gabriel N. Gatica‡ Ricardo Oyarzúa§

Abstract

In this paper we undertake an a posteriori error analysis along with its adaptive computation of a new augmented fully–mixed finite element method that we have recently proposed to numerically simulate heat driven flows in the Boussinesq approximation setting. Our approach incorporates as additional unknowns a modified pseudostress tensor field and an auxiliary vector field in the fluid and heat equations, respectively, which possibilitates the elimination of the pressure. This unknown, however, can be easily recovered by a postprocessing formula. In turn, redundant Galerkin terms are included into the weak formulation to ensure well-posedness. In this way, the resulting variational formulation is a four-field augmented scheme, whose Galerkin discretization allows a Raviart-Thomas approximation for the auxiliary unknowns and a Lagrange approximation for the velocity and the temperature. In the present work, we propose a reliable and efficient, fully-local and computable, residual–based a posteriori error estimator in two and three dimensions for the aforementioned method. Standard arguments based on duality techniques, stable Helmholtz decompositions, and well–known results from previous works, are the main underlying tools used in our methodology. Several numerical experiments illustrate the properties of the estimator and further validate the expected behaviour of the associated adaptive algorithm.

Key words: Boussinesq model, finite element method, augmented fully–mixed formulation, a posteriori analysis, reliability, efficiency, adaptive algorithm.

Mathematics subject classifications (2000): 65N30, 65N12, 65N15, 35Q79, 80A20, 76R05, 76D07

1 Introduction

We have recently analyzed in [11] the solvability and numerical approximation of a new variational formulation for the stationary Boussinesq problem modelling natural convection. There, an augmented fully-mixed formulation was introduced where a pseudostress tensor, linking the velocity with the convective term, and a vector field involving the temperature, its gradient and the velocity, are introduced as auxiliary unknowns. Then, using the incompressibility of the fluid, the pressure is eliminated, and

*This work was partially supported by CONICYT-Chile through BASAL project CMM, Universidad de Chile, project Anillo ACT1118 (ANANUM), and project Fondecyt 11121347, and the Becas–Chile programme for foreign students; by Centro de Investigación en Ingeniería Matemática (CI^{2}MA), Universidad de Concepción; and by Universidad del Bío-Bío through DIUBB project 120808 GI/EF.

†Departamento de Ciencias Básicas, Facultad de Ciencias, Universidad del Bío-Bío, Campus Fernando May, Chillán, Chile, email: ecolmenares@ubiobio.cl.

‡CI^{2}MA and Departamento de Ingeniería Matemática, Universidad de Concepción, Casilla 160-C, Concepción, Chile, email: ggatica@ci2ma.udec.cl.

§GIMNAP-Departamento de Matemática, Universidad del Bío-Bío, Casilla 5-C, Concepción, Chile, and CI^{2}MA, Universidad de Concepción, Casilla 160-C, Concepción, Chile, email: royarzua@ubiobio.cl.

as a result, a four-field system of equations is derived, where the aforementioned auxiliary variables, along with the velocity and the temperature of the fluid, are the main unknowns of the system of equations. The resulting variational formulation is enriched with Galerkin-type terms arising from the constitutive and equilibrium equations, and the Dirichlet boundary conditions, allowing the utilization of the Lax-Milgram Lemma and a fixed-point strategy (see also [13]) to prove the unique solvability of the problem. At the discrete level, this new augmented fully-mixed formulation allows the utilization of the same family of finite element subspaces for approximating the unknowns of both, the Navier-Stokes and convection-diffusion equations, which constitutes a significant advantage from a practical point of view since it permits to unify and simplify the computational implementation of the resulting discrete scheme. In particular, Raviart-Thomas spaces of order k for the auxiliary unknowns and continuous piecewise polynomials of degree $\leq k+1$ for the velocity and the temperature can be utilized yielding optimal convergence. The work [11] described above, extends the results obtained in [12], where an augmented primal-mixed approach for the stationary Boussinesq model was proposed. The name primal-mixed means that a primal formulation with a Lagrange multiplier (to impose weakly the Dirichlet boundary condition) is considered for the convection–diffusion equations whereas the same augmented mixed approach utilized in [11] is employed for the Navier-Stokes equations. We emphasize that, differently from the scheme in [12], no boundary unknowns (Lagrange multipliers) are needed in [11], which leads to an improvement of the method from both, theoretical and computational point of view.

On the other hand, residual-based a posteriori error estimators are mathematical tools typically used to guide adaptive mesh refinement in order to reduce the computational cost and also guarantee an adequate convergence behavior of the Galerkin approximations of linear as well as nonlinear boundary value problems, even under the eventual presence of singularities. In general, a global estimator $\boldsymbol{\theta}$ depends on local estimators $\boldsymbol{\theta}_T$ defined on each element T of a given mesh $\mathcal{T}_h$. Then, $\boldsymbol{\theta}$ is said to be efficient (resp. reliable) if there exists a constant $C_{\mathtt{eff}} > 0$ (resp. $C_{\mathtt{rel}} > 0$), independent of meshsizes, such that

$$C_{\mathtt{eff}}\boldsymbol{\theta} + \text{h.o.t} \leq \|error\| \leq C_{\mathtt{rel}}\boldsymbol{\theta} + \text{h.o.t},$$

where h.o.t. is a generic expression denoting one or several terms of higher order. In particular, the a posteriori error analysis of mixed variational formulations has already been widely investigated by many authors (see, e.g. [1, 2, 4, 5, 8, 20, 21, 23, 25], and the references therein). These contributions refer mainly to reliable and efficient a posteriori error estimators based on local and global residuals, local problems, postprocessing, and functional-type error estimates. In addition, the applications include the Stokes and Navier-Stokes equations, Poisson problem, linear elasticity, and general elliptic partial differential equations of second order. Nevertheless, only a couple of adaptive numerical techniques based on a posteriori error estimators have been proposed in the literature for the Boussinesq problem, and essentially for primal schemes only (see [3, 29]). The only previous contribution dealing with mixed formulations and adaptive refinements is [17], where the authors introduce appropriate refinement rules to recover the quasi-optimality of the method proposed in [16] under the presence of singular behaviours near non-convex corner points. Up to our knowledge, the first a posteriori error analysis for the Boussinesq problem, using a mixed approach for the Navier-Stokes equations, has been provided recently in [10]. There, a reliable and efficient residual-based a posteriori error estimator for the method analyzed in [12] is derived, which turns to be non-local due to the presence of the $H^{1/2}$-norm of a residual term involving the temperature on the boundary. Partially following known approaches, the proof of reliability in [10] makes use of continuous inf–sup conditions, a stable Helmholtz decomposition and the local approximation properties of the Clément and Raviart–Thomas operators. In addition, inverse inequalities, and the localization technique based on element–bubble and edge–bubble functions, are the main tools for proving the efficiency of the estimator.

Motivated by the discussion above, our goal in this paper is to additionally contribute in the direction of [10] and provide the a posteriori error analysis of the augmented fully–mixed variational approach introduced in [11]. More precisely, here we introduce a residual–based a posteriori error indicator for the method proposed in [11] which, differently to the estimator provided in [10], is fully–local and fully–computable. The rest of this work is organized as follows. In Section 2, we first recall from [11] the model problem and the corresponding augmented fully–mixed formulation as well as the associated Galerkin scheme. In Section 3, we derive the reliable and efficient residual–based a posteriori error estimator for our Galerkin scheme in two dimensions and its three–dimensional counterpart is provided in Section 4. Finally, in Section 5 we show some numerical results confirming the reliability and efficiency of the estimator, and illustrating the good performance of the associated adaptive algorithm for our finite element method.

We end this section by recalling some definitions and fixing useful notations. Given the vector fields $\boldsymbol{v} = (v_i)_{i=1,n}$ and $\boldsymbol{w} = (w_i)_{i=1,n}$, with $n \in \{2,3\}$, we set the gradient, divergence, and tensor product operators, by

$$\nabla \boldsymbol{v} := \left(\frac{\partial v_i}{\partial x_j} \right)_{i,j=1,n}, \quad \mathrm{div}\, \boldsymbol{v} := \sum_{j=1}^{n} \frac{\partial v_j}{\partial x_j}, \quad \text{and} \quad \boldsymbol{v} \otimes \boldsymbol{w} := (v_i w_j)_{i,j=1,n}.$$

Furthermore, for any tensor fields $\boldsymbol{\tau} := (\tau_{ij})_{i,j=1,n}$ and $\boldsymbol{\zeta} := (\zeta_{ij})_{i,j=1,n}$, we define the transpose, the trace, the tensor inner product, and the deviatoric tensor, respectively, by

$$\boldsymbol{\tau}^t := (\tau_{ji})_{i,j=1,n}, \quad \mathrm{tr}(\boldsymbol{\tau}) := \sum_{i=1}^{n} \tau_{ii}, \quad \boldsymbol{\tau} : \boldsymbol{\zeta} := \sum_{i,j=1}^{n} \tau_{ij}\zeta_{ij}, \quad \text{and} \quad \boldsymbol{\tau}^{\mathtt{d}} := \boldsymbol{\tau} - \frac{1}{n}\mathrm{tr}(\boldsymbol{\tau})\mathbb{I},$$

where $\mathbb{I}$ is the identity matrix in $\mathbb{R}^{n\times n}$. When no confusion arises, $|\cdot|$ will denote the Euclidean norm in $\mathbb{R}^n$ or $\mathbb{R}^{n\times n}$. Additionally, we will utilize standard simplified terminology for Sobolev spaces and norms. In particular, if $\mathcal{O}$ is a domain, Γ is an open or closed Lipschitz curve (respectively surface in $\mathbb{R}^3$), and $r \in \mathbb{R}$, we define

$$\mathbf{H}^r(\mathcal{O}) := [\mathrm{H}^r(\mathcal{O})]^n, \quad \mathbb{H}^r(\mathcal{O}) := [\mathrm{H}^r(\mathcal{O})]^{n\times n}, \quad \text{and} \quad \mathbf{H}^r(\Gamma) := [\mathrm{H}^r(\Gamma)]^n,$$

and adopt the usual convention of writing $\mathbf{L}^2(\mathcal{O}), \mathbb{L}^2(\mathcal{O})$, and $\mathbf{L}^2(\Gamma)$ instead of $\mathbf{H}^0(\mathcal{O}), \mathbb{H}^0(\mathcal{O})$, and $\mathbf{H}^0(\Gamma)$, respectively. The corresponding norms are denoted by $\|\cdot\|_{r,\mathcal{O}}$ for $\mathrm{H}^r(\mathcal{O})$, $\mathbf{H}^r(\mathcal{O})$ and $\mathbb{H}^r(\mathcal{O})$, and $\|\cdot\|_{r,\Gamma}$ for $\mathrm{H}^r(\Gamma)$ and $\mathbf{H}^r(\Gamma)$. We also write $|\cdot|_{r,\mathcal{O}}$ for the $\mathbf{H}^r$-seminorm. In addition, we recall that

$$\mathbf{H}(\mathrm{div};\mathcal{O}) := \left\{ \boldsymbol{w} \in \mathbf{L}^2(\mathcal{O}) : \quad \mathrm{div}\boldsymbol{w} \in \mathrm{L}^2(\mathcal{O}) \right\},$$

is a standard Hilbert space (see, e.g. [7, 26]), and the space of matrix valued functions whose rows belong to $\mathbf{H}(\mathrm{div};\mathcal{O})$ will be denoted by $\mathbb{H}(\mathbf{div};\mathcal{O})$. The norms of $\mathbf{H}(\mathrm{div};\mathcal{O})$ and $\mathbb{H}(\mathbf{div};\mathcal{O})$ are denoted by $\|\cdot\|_{\mathrm{div},\mathcal{O}}$ and $\|\cdot\|_{\mathbf{div},\mathcal{O}}$, respectively. Note also that $\mathbb{H}(\mathbf{div};\mathcal{O})$ can be characterized as the space of matrix valued functions $\boldsymbol{\tau}$ such that $\mathbf{c}^t\boldsymbol{\tau} \in \mathbf{H}(\mathrm{div};\mathcal{O})$ for any constant column vector $\mathbf{c}$. In addition, it is easy to see that there holds:

$$\mathbb{H}(\mathbf{div};\mathcal{O}) \;=\; \mathbb{H}_0(\mathbf{div};\mathcal{O}) \;\oplus\; \mathrm{P}_0(\mathcal{O})\,\mathbb{I}\,,$$

where

$$\mathbb{H}_0(\mathbf{div};\mathcal{O}) \;:=\; \left\{ \boldsymbol{\tau} \;\in\; \mathbb{H}(\mathbf{div};\mathcal{O}) : \quad \int_{\mathcal{O}} \mathrm{tr}\boldsymbol{\tau} = 0 \right\}$$

and $\mathrm{P}_0(\mathcal{O})$ is the space of constant polynomials on $\mathcal{O}$. More precisely, each $\boldsymbol{\tau} \in \mathbb{H}(\mathbf{div};\mathcal{O})$ can be decomposed uniquely as:

$$\boldsymbol{\tau} \,=\, \boldsymbol{\tau}_0 \,+\, c\,\mathbb{I}\,, \quad \text{with} \quad \boldsymbol{\tau}_0 \,\in\, \mathbb{H}_0(\mathbf{div};\mathcal{O}) \quad \text{and} \quad c \,:=\, \frac{1}{n\,|\mathcal{O}|}\int_{\mathcal{O}} \mathrm{tr}\,\boldsymbol{\tau} \,\in\, \mathbb{R}\,.$$

Such a decomposition will be exploited in the subsequent analysis of weak formulations.

Furthermore, given an integer $k \geq 0$ and a set $M \subseteq \mathbb{R}^n$, $\mathrm{P}_k(M)$ denotes the space of polynomials on M of degree $\leq k$. In addition, we set $\mathbf{P}_k(M) := [\mathrm{P}_k(M)]^n$ and $\mathbb{P}_k(M) := [\mathrm{P}_k(M)]^{n\times n}$. Finally, throughout the rest of the paper, we employ $\mathbf{0}$ to denote a generic null vector (including the null functional and operator), and use C and c, with or without subscripts, bars, tildes or hats, to denote generic constants independent of the discretization, which may take different values at different places.

2 The stationary Boussinesq problem

2.1 The model problem

Let $\Omega \in \mathbb{R}^n$, with $n \in \{2,3\}$, be a bounded domain with Lipschitz–boundary Γ. Then the Boussinesq problem is given by the nonlinear, coupled system of partial differential equations

$$\begin{aligned} -\,\mu\,\Delta\boldsymbol{u} \,+\, (\nabla\boldsymbol{u})\,\boldsymbol{u} \,+\, \nabla p \,-\, \varphi\,\boldsymbol{g} \,=\, 0\,, \qquad \mathrm{div}\,\boldsymbol{u} \,=\, 0 \quad \text{in} \quad \Omega\,, \\ -\,\mathrm{div}(\mathbb{K}\,\nabla\varphi) \,+\, \boldsymbol{u}\cdot\nabla\varphi \,=\, 0 \quad \text{in} \quad \Omega\,, \end{aligned} \tag{2.1}$$

where the unknowns are the velocity $\boldsymbol{u}$, the pressure p and the temperature φ of a fluid occupying the region Ω. We prescribe the Dirichlet boundary conditions

$$\boldsymbol{u} \,=\, \boldsymbol{u}_D\,, \quad \text{and} \quad \varphi \,=\, \varphi_D \quad \text{on} \quad \Gamma\,, \tag{2.2}$$

with $\boldsymbol{u}_D \in \mathbf{H}^{1/2}(\Gamma)$ and $\varphi_D \in \mathrm{H}^{1/2}(\Gamma)$. The rest of data we consider are the gravitational force $\boldsymbol{g} \in \mathbf{L}^\infty(\Omega)$, the fluid viscosity $\mu > 0$, and the uniformly positive definite tensor $\mathbb{K} \in \mathbb{L}^\infty(\Omega)$, describing the thermal conductivity and satisfying

$$\mathbb{K}^{-1}\,\boldsymbol{c}\cdot\boldsymbol{c} \,\geq\, \kappa_0\,|\boldsymbol{c}|^2 \quad \forall\,\boldsymbol{c} \,\in\, \mathbb{R}^n\,,$$

where κ_0 is some positive constant. As usual, the Dirichlet datum $\boldsymbol{u}_D$ must satisfy the compatibility condition

$$\int_\Gamma \boldsymbol{u}_D\cdot\boldsymbol{\nu} = 0\,,$$

which is forced by the incompressibility condition. In addition, it is well known that the uniqueness of a pressure solution of (2.1) is ensured in the space $\mathrm{L}^2_0(\Omega) \,=\, \Big\{\, q \,\in\, \mathrm{L}^2(\Omega) \,:\, \int_\Omega q \,=\, 0 \Big\}$.

Now to derive our mixed approach we include as auxiliary variables the pseudostress tensor $\boldsymbol{\sigma}$ and the vector $\mathbf{p}$ defined, respectively, by

$$\boldsymbol{\sigma} \,:=\, \mu\,\nabla\boldsymbol{u} \,-\, (\boldsymbol{u}\otimes\boldsymbol{u}) \,-\, p\,\mathbb{I}\,, \quad \text{and} \quad \mathbf{p} \,:=\, \mathbb{K}\,\nabla\varphi \,-\, \varphi\,\boldsymbol{u} \quad \text{in} \quad \Omega\,,$$

and rewrite (2.1)–(2.2) equivalently as the set of first order equations (see [11, Section 2]):

$$\begin{gathered}\mu\,\nabla\boldsymbol{u}\,-\,(\boldsymbol{u}\otimes\boldsymbol{u})^{\mathtt{d}}\,=\,\boldsymbol{\sigma}^{\mathtt{d}}\quad\text{in}\quad\Omega,\quad-\,\mathbf{div}(\boldsymbol{\sigma})\,-\,\varphi\,\boldsymbol{g}\,=\,0\quad\text{in}\quad\Omega,\\ \mathbb{K}^{-1}\,\mathbf{p}\,+\,\mathbb{K}^{-1}\,\varphi\,\boldsymbol{u}\,=\,\nabla\varphi\quad\text{in}\quad\Omega,\quad\mathrm{div}(\mathbf{p})\,=\,0\quad\text{in}\quad\Omega,\\ \boldsymbol{u}\,=\,\boldsymbol{u}_D\quad\text{on}\quad\Gamma,\quad\varphi\,=\,\varphi_D\quad\text{on}\quad\Gamma\quad\text{and}\quad\int_\Omega\mathrm{tr}(\boldsymbol{\sigma}\,+\,\boldsymbol{u}\otimes\boldsymbol{u})\,=\,0\,.\end{gathered}\tag{2.3}$$

Note from the definition of $\boldsymbol{\sigma}$ and the incompressibility condition of the fluid, that the pressure p can be recovered in terms of $\boldsymbol{\sigma}$ and $\boldsymbol{u}$ as follows

$$p\,=\,-\frac{1}{n}\,\mathrm{tr}(\,\boldsymbol{\sigma}+\boldsymbol{u}\otimes\boldsymbol{u}\,)\quad\text{in}\quad\Omega\,.$$

2.2 The augmented fully–mixed variational formulation

Proceeding as in [11], that is, multiplying equations (2.3) by suitable test functions, integrating by parts, utilizing the Dirichlet boundary conditions, and adding the Galerkin type terms

$$\begin{aligned}\kappa_1\int_\Omega\Big(\mu\,\nabla\boldsymbol{u}\,-\,\boldsymbol{\sigma}^{\mathtt{d}}\,-\,(\boldsymbol{u}\otimes\boldsymbol{u})^{\mathtt{d}}\Big)\,:\,\nabla\boldsymbol{v}\;&=\;0\qquad&&\forall\,\boldsymbol{v}\,\in\,\mathbf{H}^1(\Omega)\,,\\ \kappa_2\int_\Omega\mathbf{div}\,\boldsymbol{\sigma}\cdot\mathbf{div}\,\boldsymbol{\tau}\,+\,\kappa_2\int_\Omega\varphi\,\boldsymbol{g}\cdot\mathbf{div}\,\boldsymbol{\tau}\;&=\;0\qquad&&\forall\,\boldsymbol{\tau}\,\in\,\mathbb{H}_0(\mathbf{div};\Omega)\,,\\ \kappa_3\int_\Gamma\boldsymbol{u}\cdot\boldsymbol{v}\;&=\;\kappa_3\int_\Gamma\boldsymbol{u}_D\cdot\boldsymbol{v}\qquad&&\forall\,\boldsymbol{v}\,\in\,\mathbf{H}^1(\Omega)\,,\end{aligned}$$

and

$$\begin{aligned}\kappa_4\int_\Omega\Big(\mathbb{K}^{-1}\,\mathbf{p}\,-\,\nabla\varphi\,+\,\mathbb{K}^{-1}\varphi\,\boldsymbol{u}\Big)\cdot\nabla\psi\;&=\;0\qquad&&\forall\,\psi\,\in\,\mathrm{H}^1(\Omega)\,,\\ \kappa_5\int_\Omega\mathrm{div}\,\mathbf{p}\,\mathrm{div}\,\mathbf{q}\;&=\;0\qquad&&\forall\,\mathbf{q}\,\in\,\mathbf{H}(\mathrm{div};\Omega)\,,\\ \kappa_6\int_\Gamma\varphi\,\psi\;&=\;\kappa_6\int_\Gamma\varphi_D\,\psi\qquad&&\forall\,\psi\,\in\,\mathrm{H}^1(\Omega)\,,\end{aligned}$$

where $(\kappa_1\,,\,\ldots\,,\,\kappa_6)$ is a vector of positive parameters to be suitably chosen (see Theorem 2.1 below), we arrive at the variational problem: Find $(\,\boldsymbol{\sigma},\,\boldsymbol{u},\,\mathbf{p},\,\varphi\,)\,\in\,\mathbb{H}_0(\mathbf{div};\Omega)\times\mathbf{H}^1(\Omega)\times\mathbf{H}(\mathrm{div};\Omega)\times\mathrm{H}^1(\Omega)$, such that

$$\begin{aligned}\mathbf{A}((\boldsymbol{\sigma},\boldsymbol{u}),(\boldsymbol{\tau},\boldsymbol{v}))+\mathbf{B}_{\boldsymbol{u}}((\boldsymbol{\sigma},\boldsymbol{u}),(\boldsymbol{\tau},\boldsymbol{v}))\;&=\;\big(F_\varphi+F_D\big)(\boldsymbol{\tau},\boldsymbol{v})\quad\forall\,(\boldsymbol{\tau},\boldsymbol{v})\in\mathbb{H}_0(\mathbf{div};\Omega)\times\mathbf{H}^1(\Omega)\,,\\ \widetilde{\mathbf{A}}((\mathbf{p},\varphi),(\mathbf{q},\psi))+\widetilde{\mathbf{B}}_{\boldsymbol{u}}((\mathbf{p},\varphi),(\mathbf{q},\psi))\;&=\;\widetilde{F}_D(\mathbf{q},\psi)\qquad\forall\,(\mathbf{q},\psi)\in\mathbf{H}(\mathrm{div};\Omega)\times\mathrm{H}^1(\Omega)\,,\end{aligned}\tag{2.4}$$

where the forms $\mathbf{A}$, $\mathbf{B}_{\boldsymbol{w}}$, $\widetilde{\mathbf{A}}$, and $\widetilde{\mathbf{B}}_{\boldsymbol{w}}$ are defined, respectively, as

$$\begin{aligned}\mathbf{A}(\,(\boldsymbol{\sigma},\boldsymbol{u})\,,\,(\boldsymbol{\tau},\boldsymbol{v})\,)\,:=\,&\int_\Omega\boldsymbol{\sigma}^{\mathtt{d}}:(\,\boldsymbol{\tau}^{\mathtt{d}}\,-\,\kappa_1\,\nabla\boldsymbol{v}\,)\,+\int_\Omega(\,\mu\,\boldsymbol{u}\,+\,\kappa_2\,\mathbf{div}(\boldsymbol{\sigma})\,)\cdot\mathbf{div}(\boldsymbol{\tau})\\ &-\;\mu\int_\Omega\boldsymbol{v}\cdot\mathbf{div}(\boldsymbol{\sigma})\,+\,\mu\,\kappa_1\int_\Omega\nabla\boldsymbol{u}:\nabla\boldsymbol{v}+\kappa_3\int_\Gamma\boldsymbol{u}\cdot\boldsymbol{v}\,,\end{aligned}\tag{2.5}$$

$$\mathbf{B}_{\boldsymbol{w}}(\,(\boldsymbol{\sigma},\boldsymbol{u})\,,\,(\boldsymbol{\tau},\boldsymbol{v})\,)\,:=\,\int_\Omega(\boldsymbol{u}\otimes\boldsymbol{w})^{\mathtt{d}}:(\,\boldsymbol{\tau}^{\mathtt{d}}\,-\,\kappa_1\,\nabla\boldsymbol{v}\,)\,,\tag{2.6}$$

$$\begin{aligned}\widetilde{\mathbf{A}}(\,(\mathbf{p},\varphi)\,,\,(\mathbf{q},\psi)\,)\,:=\,&\int_\Omega\mathbb{K}^{-1}\,\mathbf{p}\cdot(\,\mathbf{q}\,-\,\kappa_4\,\nabla\psi\,)\,+\int_\Omega(\,\varphi\,+\,\kappa_5\,\mathrm{div}(\mathbf{p})\,)\,\mathrm{div}(\mathbf{q})\\ &-\;\int_\Omega\psi\,\mathrm{div}(\mathbf{p})\,+\,\kappa_4\int_\Omega\nabla\varphi\cdot\nabla\psi\,+\,\kappa_6\int_\Gamma\varphi\,\psi\,,\end{aligned}\tag{2.7}$$

and

$$\widetilde{\mathbf{B}}_{\boldsymbol{w}}(\,(\mathbf{p},\varphi)\,,\,(\mathbf{q},\psi)\,)\,:=\,\int_\Omega \mathbb{K}^{-1}\,\varphi\,\boldsymbol{w}\cdot(\,\mathbf{q}\,-\,\kappa_4\nabla\psi\,), \tag{2.8}$$

for all $(\boldsymbol{\sigma},\boldsymbol{u})\,,(\boldsymbol{\tau},\boldsymbol{v})\,\in\,\mathbb{H}_0(\mathbf{div};\Omega)\,\times\,\mathbf{H}^1(\Omega)$, for all $(\mathbf{p},\varphi)\,,(\mathbf{q},\psi)\,\in\,\mathbf{H}(\mathrm{div};\Omega)\,\times\,\mathrm{H}^1(\Omega)$, and for all $\boldsymbol{w}\,\in\,\mathbf{H}^1(\Omega)$. Note that $\mathbf{A}$ and $\widetilde{\mathbf{A}}$ are bilinear as well as $\mathbf{B}_{\boldsymbol{w}}$ and $\widetilde{\mathbf{B}}_{\boldsymbol{w}}$ (for a fixed $\boldsymbol{w}\,\in\,\mathbf{H}^1(\Omega)$). In addition, given $\varphi\,\in\,\mathrm{H}^1(\Omega)$, F_φ, F_D, and $\widetilde{F}_D$ are the bounded linear functionals given by

$$F_\varphi(\boldsymbol{\tau},\boldsymbol{v})\,:=\,\int_\Omega \varphi\,\mathbf{g}\cdot(\,\mu\,\boldsymbol{v}\,-\,\kappa_2\,\mathbf{div}(\boldsymbol{\tau})\,)\quad\forall\,(\boldsymbol{\tau},\boldsymbol{v})\,\in\,\mathbb{H}_0(\mathbf{div};\Omega)\,\times\,\mathbf{H}^1(\Omega)\,, \tag{2.9}$$

$$F_D(\boldsymbol{\tau},\boldsymbol{v})\,:=\,\kappa_3\,\int_\Gamma \boldsymbol{u}_D\cdot\boldsymbol{v}\,+\,\mu\,\langle\,\boldsymbol{\tau}\boldsymbol{\nu}\,,\boldsymbol{u}_D\,\rangle_\Gamma\quad\forall\,(\boldsymbol{\tau},\boldsymbol{v})\,\in\,\mathbb{H}_0(\mathbf{div};\Omega)\,\times\,\mathbf{H}^1(\Omega)\,, \tag{2.10}$$

and

$$\widetilde{F}_D(\mathbf{q},\psi)\,:=\,\kappa_6\,\int_\Gamma \varphi_D\,\psi\,+\,\langle\,\mathbf{q}\cdot\boldsymbol{\nu}\,,\varphi_D\,\rangle_\Gamma\quad\forall\,(\mathbf{q},\psi)\,\in\,\mathbf{H}(\mathrm{div};\Omega)\,\times\,\mathrm{H}^1(\Omega)\,. \tag{2.11}$$

As explained in [11, 12] it is possible to prove that the forms above satisfy:

$$|\mathbf{A}(\,(\boldsymbol{\sigma},\boldsymbol{u})\,,\,(\boldsymbol{\tau},\boldsymbol{v})\,)|\,\leq\|\mathbf{A}\|\,\|(\boldsymbol{\sigma},\boldsymbol{u})\|\,\|(\boldsymbol{\tau},\boldsymbol{v})\|\,, \tag{2.12}$$

$$|\widetilde{\mathbf{A}}(\,(\mathbf{p},\varphi)\,,\,(\mathbf{q},\psi)\,)|\,\leq\|\widetilde{\mathbf{A}}\|\,\|(\mathbf{p},\varphi)\|\,\|(\mathbf{q},\psi)\|\,, \tag{2.13}$$

$$|\mathbf{B}_{\boldsymbol{w}}((\boldsymbol{\sigma},\boldsymbol{u}),(\boldsymbol{\tau},\boldsymbol{v}))|\,\leq c_1(\Omega)\,(\,\kappa_1^2\,+\,1\,)^{1/2}\,\|\boldsymbol{w}\|_{1,\Omega}\,\|\boldsymbol{u}\|_{1,\Omega}\,\|(\boldsymbol{\tau},\boldsymbol{v})\|, \tag{2.14}$$

$$|\widetilde{\mathbf{B}}_{\boldsymbol{w}}(\,(\mathbf{p},\varphi)\,,\,(\mathbf{q},\psi)\,)|\,\leq(\kappa_4^2\,+\,1\,)^{1/2}\,\|\mathbb{K}^{-1}\|_{\infty,\Omega}\,c_2(\Omega)\,\|\boldsymbol{w}\|_{1,\Omega}\,\|\varphi\|_{1,\Omega}\,\|(\mathbf{q},\psi)\|\,, \tag{2.15}$$

for all $(\boldsymbol{\sigma},\boldsymbol{u})\,,(\boldsymbol{\tau},\boldsymbol{v})\,\in\,\mathbb{H}_0(\mathbf{div};\Omega)\,\times\,\mathbf{H}^1(\Omega)$, $(\mathbf{p},\varphi)\,,(\mathbf{q},\psi)\,\in\,\mathbf{H}(\mathrm{div};\Omega)\,\times\,\mathrm{H}^1(\Omega)$, and for all $\boldsymbol{w}\,\in\,\mathbf{H}^1(\Omega)$. In (2.14) and (2.15) the constants $c_1(\Omega)$ and $c_2(\Omega)$ depend only on Ω, whereas in (2.12) and (2.13) the constants $\|\mathbf{A}\|$ and $\|\widetilde{\mathbf{A}}\|$, denoting the norms of the bounded linear operators induced by the respective bilinear forms, depend on Ω, the physical parameters μ and $\mathbb{K}$, and the constants κ_i, $i\,\in\,\{1,\ldots,6\}$. Furthermore, it can be also proved that $\mathbf{A}$ and $\widetilde{\mathbf{A}}$ are strongly elliptic. In fact, for $\mathbf{A}$ we have that for each $\kappa_1\,\in\,(0,\,2\,\delta)$, with $\delta\,\in\,(0,\,2\,\mu)$, and $\kappa_2\,,\kappa_3\,>\,0$, there exists a positive constant $\alpha(\Omega)$, depending only on μ, κ_1, κ_2, κ_3, and Ω, such that (see [12, Lemma 3.3] for details)

$$\mathbf{A}(\,(\boldsymbol{\tau},\boldsymbol{v})\,,\,(\boldsymbol{\tau},\boldsymbol{v})\,)\,\geq\,\alpha(\Omega)\,\|(\boldsymbol{\tau},\boldsymbol{v})\|^2\quad\forall\,(\boldsymbol{\tau},\boldsymbol{v})\,\in\,\mathbb{H}_0(\mathbf{div};\Omega)\,\times\,\mathbf{H}^1(\Omega),$$

whereas if $\kappa_4\,\in\,\Big(0,\,\dfrac{2\,\kappa_0\,\widetilde{\delta}}{\|\mathbb{K}^{-1}\|_{\infty,\Omega}}\Big)$, with $\widetilde{\delta}\,\in\,\Big(0,\,\dfrac{2}{\|\mathbb{K}^{-1}\|_{\infty,\Omega}}\Big)$, and κ_5, $\kappa_6\,>\,0$, for $\widetilde{\mathbf{A}}$ we deduce that there exists $\widetilde{\alpha}(\Omega)\,>\,0$, depending only on $\mathbb{K}$, κ_4, κ_5, κ_6 and Ω, such that (see [11, Lemma 3.3] for details)

$$\widetilde{\mathbf{A}}(\,(\mathbf{q},\psi)\,,\,(\mathbf{q},\psi)\,)\,\geq\,\widetilde{\alpha}(\Omega)\,\|(\mathbf{q},\psi)\|^2\quad\forall\,(\mathbf{q},\psi)\,\in\,\mathbf{H}(\mathrm{div};\Omega)\,\times\,\mathrm{H}^1(\Omega).$$

The following result taken from [11] establishes the well-posedness of (2.4).

Theorem 2.1 *Let* $\kappa_1\,\in\,(0,\,2\,\delta)$, *with* $\delta\,\in\,(0,\,2\,\mu)$, $\kappa_4\,\in\,\Big(0,\,\dfrac{2\,\kappa_0\,\widetilde{\delta}}{\|\mathbb{K}^{-1}\|_{\infty,\Omega}}\Big)$, *with* $\widetilde{\delta}\,\in\,\Big(0,\,\dfrac{2}{\|\mathbb{K}^{-1}\|_{\infty,\Omega}}\Big)$, *and* κ_2, κ_3, κ_5, $\kappa_6\,>\,0$. *Given* $r\,\in\,\big(0,\min\{\,r_0,\widetilde{r}_0\}\big)$, *with* r_0 *and* $\widetilde{r}_0$ *given by*

$$r_0\,:=\,\frac{\alpha(\Omega)}{2\,(\,\kappa_1^2\,+\,1)^{1/2}\,c_1(\Omega)}\quad\textit{and}\quad\widetilde{r}_0\,:=\,\frac{\widetilde{\alpha}(\Omega)}{2\,(\,\kappa_4^2\,+\,1\,)^{1/2}\,\|\mathbb{K}^{-1}\|_{\infty,\Omega}\,c_2(\Omega)}, \tag{2.16}$$

respectively, let $\mathbf{W}_r := \Big\{ (\boldsymbol{w},\phi) \in \mathbf{H} : \quad \|(\boldsymbol{w},\phi)\| \leq r \Big\}$, *and assume that the data* $\boldsymbol{g}$, $\boldsymbol{u}_D$, *and* φ_D *satisfy*

$$c_{\mathbf{S}} \Big\{ r\,\|\boldsymbol{g}\|_{\infty,\Omega} + \|\boldsymbol{u}_D\|_{0,\Gamma} + \|\boldsymbol{u}_D\|_{1/2,\Gamma} \Big\} + c_{\widetilde{\mathbf{S}}} \Big\{ \|\varphi_D\|_{0,\Gamma} + \|\varphi_D\|_{1/2,\Gamma} \Big\} \leq r\,. \tag{2.17}$$

and

$$C_{\mathbf{T}} \Big(\|\boldsymbol{g}\|_{\infty,\Omega} + c_{\mathbf{S}} \Big\{ r\,\|\boldsymbol{g}\|_{\infty,\Omega} + \|\boldsymbol{u}_D\|_{0,\Gamma} + \|\boldsymbol{u}_D\|_{1/2,\Gamma} \Big\} \Big) < 1\,, \tag{2.18}$$

where $c_{\mathbf{S}}$, $c_{\widetilde{\mathbf{S}}}$ *and* $C_{\mathbf{T}}$ *are the positive constants in* [11, Lemma 3.1], [11, Lemma 3.3] *and* [11, Lemma 3.8], *respectively. Then, there exists a unique* $(\boldsymbol{\sigma},\boldsymbol{u},\mathbf{p},\varphi) \in \mathbb{H}_0(\mathbf{div};\Omega) \times \mathbf{H}^1(\Omega) \times \mathbf{H}(\mathrm{div};\Omega) \times \mathrm{H}^1(\Omega)$ *solution to* (2.4), *with* $(\boldsymbol{u},\varphi) \in \mathbf{W}_r$. *Moreover, there holds*

$$\|(\boldsymbol{\sigma},\boldsymbol{u})\| \leq c_{\mathbf{S}} \Big\{ r\,\|\boldsymbol{g}\|_{\infty,\Omega} + \|\boldsymbol{u}_D\|_{0,\Gamma} + \|\boldsymbol{u}_D\|_{1/2,\Gamma} \Big\}\,,$$

and

$$\|(\mathbf{p},\varphi)\| \leq c_{\widetilde{\mathbf{S}}} \Big\{ \|\varphi_D\|_{0,\Gamma} + \|\varphi_D\|_{1/2,\Gamma} \Big\}\,.$$

2.3 The augmented fully–mixed finite element method

Here, for clarity of exposition of the a posteriori error estimator to be defined next in Section 3, we introduce a Galerkin scheme of (2.4) by restricting ourselves to the particular case provided in [11, Section 4.3]. To that end, we let $\mathcal{T}_h$ be a regular triangulation of $\overline{\Omega}$ consisting of triangles/tetrahedra of diameter h_T, and meshsize $h := \max \Big\{ h_T : \quad T \in \mathcal{T}_h \Big\}$, consider an integer $k \geq 0$, and for each $T \in \mathcal{T}_h$ we denote by

$$\mathbf{RT}_k(T) := \mathbf{P}_k(T) + \mathrm{P}_k(T)\,\boldsymbol{x}\,,$$

the local Raviart–Thomas space of order k, where, according to the notations described in the Section 1, $\mathbf{P}_k(T) := [\mathrm{P}_k(T)]^n$, and $\boldsymbol{x}$ is the generic vector in $\mathbb{R}^n$. Similarly, $\mathbf{C}(\overline{\Omega}) = [\mathrm{C}(\overline{\Omega})]^n$. Then, we introduce the finite element subspaces approximating the unknowns $\boldsymbol{\sigma}$ and $\boldsymbol{u}$ as

$$\mathbb{H}_h^{\boldsymbol{\sigma}} := \Big\{ \boldsymbol{\tau}_h \in \mathbb{H}_0(\mathbf{div};\Omega) : \quad \boldsymbol{c}^t\,\boldsymbol{\tau}_h\Big|_T \in \mathbf{RT}_k(T) \quad \forall\,\boldsymbol{c} \in \mathbb{R}^n \quad \forall\,T \in \mathcal{T}_h \Big\}\,,$$

and

$$\mathbf{H}_h^{\boldsymbol{u}} := \Big\{ \boldsymbol{v}_h \in \mathbf{C}(\overline{\Omega}) : \quad \boldsymbol{v}_h\Big|_T \in \mathbf{P}_{k+1}(T) \quad \forall\,T \in \mathcal{T}_h \Big\}.$$

In turn, we define the approximating spaces for $\mathbf{p}$ and the temperature φ as

$$\mathbf{H}_h^{\mathbf{p}} := \Big\{ \mathbf{q}_h \in \mathbf{H}(\mathrm{div};\Omega) : \quad \mathbf{q}_h\Big|_T \in \mathbf{RT}_k(T) \quad \forall\,T \in \mathcal{T}_h \Big\}$$

and

$$\mathrm{H}_h^{\varphi} := \Big\{ \psi_h \in \mathrm{C}(\overline{\Omega}) : \quad \psi_h\Big|_T \in \mathrm{P}_{k+1}(T) \quad \forall\,T \in \mathcal{T}_h \Big\}\,.$$

Then, with the forms defined through (2.5)-(2.11), the Galerkin scheme of (2.4) reads: Find $(\boldsymbol{\sigma}_h,\boldsymbol{u}_h,\mathbf{p}_h,\varphi_h) \in \mathbb{H}_h^{\boldsymbol{\sigma}} \times \mathbf{H}_h^{\boldsymbol{u}} \times \mathbf{H}_h^{\mathbf{p}} \times \mathrm{H}_h^{\varphi}$ such that

$$\begin{aligned} \mathbf{A}\big((\boldsymbol{\sigma}_h,\boldsymbol{u}_h),(\boldsymbol{\tau}_h,\boldsymbol{v}_h)\big) + \mathbf{B}_{\boldsymbol{u}_h}\big((\boldsymbol{\sigma}_h,\boldsymbol{u}_h),(\boldsymbol{\tau}_h,\boldsymbol{v}_h)\big) &= F_{\varphi_h}\big((\boldsymbol{\tau}_h,\boldsymbol{v}_h)\big) + F_D\big((\boldsymbol{\tau}_h,\boldsymbol{v}_h)\big) \\ \widetilde{\mathbf{A}}\big((\mathbf{p}_h,\varphi_h),(\mathbf{q}_h,\psi_h)\big) + \widetilde{\mathbf{B}}_{\boldsymbol{u}_h}\big((\mathbf{p}_h,\varphi_h),(\mathbf{q}_h,\psi_h)\big) &= \widetilde{F}_D\big((\mathbf{q}_h,\psi_h)\big)\,, \end{aligned} \tag{2.19}$$

for all $(\boldsymbol{\tau}_h,\boldsymbol{v}_h,\mathbf{q}_h,\psi_h) \in \mathbb{H}_h^{\boldsymbol{\sigma}} \times \mathbf{H}_h^{\boldsymbol{u}} \times \mathbf{H}_h^{\mathbf{p}} \times \mathrm{H}_h^{\varphi}$.

The following theorems, also taken from [11], provide the well–posedness of (2.19), the associated Céa estimate, and the corresponding theoretical rate of convergence.

Theorem 2.2 *Let* $\kappa_1 \in (0,\, 2\,\delta)$, *with* $\delta \in (0,\, 2\,\mu)$, $\kappa_4 \in \Big(0,\, \dfrac{2\,\kappa_0\,\widetilde{\delta}}{\|\mathbb{K}^{-1}\|_{\infty,\Omega}}\Big)$, *with* $\widetilde{\delta} \in \Big(0,\, \dfrac{2}{\|\mathbb{K}^{-1}\|_{\infty,\Omega}}\Big)$, *and* $\kappa_2,\, \kappa_3,\, \kappa_5,\, \kappa_6 > 0$. *Given* $r \in \big(0, \min\{\, r_0, \widetilde{r}_0\}\big)$, *with* r_0 *and* $\widetilde{r}_0$ *given by* (2.16), *let* $\mathbf{W}_{r,h} := \Big\{\, (\boldsymbol{w}_h, \phi_h) \in \mathbf{H}_h : \quad \|(\boldsymbol{w}_h, \phi_h)\| \leq r \,\Big\}$, *and assume that the data* $\boldsymbol{g}$, $\boldsymbol{u}_D$, *and* φ_D *satisfy* (2.17) *and* (2.18). *Then, the Galerkin scheme* (2.19) *has a unique solution* $(\boldsymbol{\sigma}_h, \boldsymbol{u}_h, \mathbf{p}_h, \varphi_h) \in \mathbb{H}_h^{\boldsymbol{\sigma}} \times \mathbf{H}_h^{\boldsymbol{u}} \times \mathbf{H}_h^{\mathbf{p}} \times \mathrm{H}_h^{\varphi}$, *with* $(\boldsymbol{u}_h, \varphi_h) \in \mathbf{W}_{r,h}$, *and there hold*

$$\|(\boldsymbol{\sigma}_h, \boldsymbol{u}_h)\| \leq c_{\mathbf{S}} \Big\{ r\, \|\boldsymbol{g}\|_{\infty,\Omega} + \|\boldsymbol{u}_D\|_{0,\Gamma} + \|\boldsymbol{u}_D\|_{1/2,\Gamma} \Big\}, \tag{2.20}$$

and

$$\|(\mathbf{p}_h, \varphi_h)\| \leq c_{\widetilde{\mathbf{S}}} \Big\{ \|\varphi_D\|_{0,\Gamma} + \|\varphi_D\|_{1/2,\Gamma} \Big\}.$$

Theorem 2.3 *Assume that the data* $\boldsymbol{g}$, $\boldsymbol{u}_D$ *and* φ_D *satisfy:*

$$\mathbf{C}_i(\boldsymbol{g}, \boldsymbol{u}_D, \varphi_D) \leq \frac{1}{2} \qquad \forall\, i \in \{1, 2\},$$

with $\mathbf{C}_1$ *and* $\mathbf{C}_2$ *be the positive constants, independent of* h, *provided in* [11, Lemma 5.3]. *Then, there exists a positive constant* C_1, *independent of* h, *such that*

$$\begin{aligned} &\|(\boldsymbol{\sigma}, \boldsymbol{u}) - (\boldsymbol{\sigma}_h, \boldsymbol{u}_h)\| + \|(\mathbf{p}, \varphi) - (\mathbf{p}_h, \varphi_h)\| \\ &\leq C_1 \left\{ \mathrm{dist}\Big((\boldsymbol{\sigma}, \boldsymbol{u}), \mathbb{H}_h^{\boldsymbol{\sigma}} \times \mathbf{H}_h^{\boldsymbol{u}}\Big) + \mathrm{dist}\Big((\mathbf{p}, \varphi), \mathbf{H}_h^{\mathbf{p}} \times \mathrm{H}_h^{\varphi}\Big) \right\}. \end{aligned}$$

Moreover, if the exists $s > 0$ *such that* $\boldsymbol{\sigma} \in \mathbb{H}^s(\Omega)$, $\mathbf{div}\, \boldsymbol{\sigma} \in \mathbf{H}^s(\Omega)$, $\boldsymbol{u} \in \mathbf{H}^{s+1}(\Omega)$, $\mathbf{p} \in \mathbf{H}^s(\Omega)$, $\mathrm{div}\, \mathbf{p} \in \mathrm{H}^s(\Omega)$, *and* $\varphi \in \mathrm{H}^{s+1}(\Omega)$, *then there exists* $C_2 > 0$, *independent of* h, *such that there holds*

$$\begin{aligned} &\|(\boldsymbol{\sigma}, \boldsymbol{u}) - (\boldsymbol{\sigma}_h, \boldsymbol{u}_h)\| + \|(\mathbf{p}, \varphi) - (\mathbf{p}_h, \varphi_h)\| \\ &\leq C_2\, h^{\min\{s, k+1\}} \Big\{ \|\boldsymbol{\sigma}\|_{s,\Omega} + \|\mathbf{div}\, \boldsymbol{\sigma}\|_{s,\Omega} + \|\boldsymbol{u}\|_{s+1,\Omega} + \|\mathbf{p}\|_{s,\Omega} + \|\mathrm{div}\, \mathbf{p}\|_{s,\Omega} + \|\varphi\|_{s+1,\Omega} \Big\}. \end{aligned}$$

3 A posteriori error estimation: the 2D–case

3.1 The residual–based error estimator

We start by introducing a few useful notations for describing local information on elements and edges. Let $\mathcal{E}_h$ be the set of edges of $\mathcal{T}_h$, and define

$$\mathcal{E}_h(\Omega) := \{\, e \in \mathcal{E}_h : \quad e \subseteq \Omega \,\} \quad \text{and} \quad \mathcal{E}_h(\Gamma) := \{\, e \in \mathcal{E}_h : \quad e \subseteq \Gamma \,\}.$$

For each $T \in \mathcal{T}_h$, we similarly denote

$$\mathcal{E}_{h,T}(\Omega) = \{\, e \subseteq \partial T : \quad e \in \mathcal{E}_h(\Omega) \,\} \quad \text{and} \quad \mathcal{E}_{h,T}(\Gamma) = \{\, e \subseteq \partial T : \quad e \in \mathcal{E}_h(\Gamma) \,\}.$$

We also define unit normal and tangential vectors $\boldsymbol{\nu}_e$ and $\boldsymbol{s}_e$, respectively, on each edge by

$$\boldsymbol{\nu}_e := (\nu_1, \nu_2)^{\mathtt{t}} \quad \text{and} \quad \boldsymbol{s}_e := (-\nu_2, \nu_1)^{\mathtt{t}} \quad \forall\, e \in \mathcal{E}_h.$$

However, when no confusion arises, we will simply write $\boldsymbol{s}$ and $\boldsymbol{\nu}$ instead of $\boldsymbol{s}_e$ and $\boldsymbol{\nu}_e$, respectively.

The usual jump operator $[\![\cdot]\!]$ across internal edges are defined for piecewise continuous matrix, vector, or scalar-valued functions $\boldsymbol{\zeta}$ by

$$[\![\boldsymbol{\zeta}]\!] \,=\, (\boldsymbol{\zeta}\big|_{T_+})|_e, -(\boldsymbol{\zeta}\big|_{T_-})|_e \quad \text{with} \quad e \,=\, \partial T_+ \cap \partial T_-,$$

where T_+ and T_- are the triangles of $\mathcal{T}_h$ having e as a common edge. In addition, given scalar, vector and matrix valued fields ϕ, $\boldsymbol{\psi} = (\psi_1, \psi_2)$ and $\boldsymbol{\zeta} = (\zeta_{i,j})_{1\leq i,j\leq 2}$, respectively, we set

$$\mathbf{curl}(\phi) \,=\, \begin{pmatrix} \frac{\partial \phi}{\partial x_2} \\ -\frac{\partial \phi}{\partial x_1} \end{pmatrix}, \quad \mathrm{rot}(\boldsymbol{\psi}) \,=\, \frac{\partial \psi_2}{\partial x_1} - \frac{\partial \psi_1}{\partial x_2} \quad \text{and} \quad \mathrm{curl}(\boldsymbol{\zeta}) \,=\, \begin{pmatrix} \frac{\partial \zeta_{12}}{\partial x_1} - \frac{\partial \zeta_{11}}{\partial x_2} \\ \frac{\partial \zeta_{22}}{\partial x_1} - \frac{\partial \zeta_{21}}{\partial x_2} \end{pmatrix},$$

where the derivatives involved are taken in the distributional sense.

Now, we let $(\,\boldsymbol{\sigma}_h,\, \boldsymbol{u}_h,\, \mathbf{p}_h,\, \varphi_h\,) \in \mathbb{H}_h^{\boldsymbol{\sigma}} \times \mathbf{H}_h^{\boldsymbol{u}} \times \mathbf{H}_h^{\mathbf{p}} \times \mathrm{H}_h^{\varphi}$ be the unique solution of (2.19) and for each $T \in \mathcal{T}_h$, we define the local indicators

$$\begin{aligned} \boldsymbol{\theta}_{T,\mathtt{f}}^2 \,:=\, & \|\mu\, \nabla \boldsymbol{u}_h - \boldsymbol{\sigma}_h^{\mathtt{d}} - (\boldsymbol{u}_h \otimes \boldsymbol{u}_h)^{\mathtt{d}}\|_{0,T}^2 \,+\, \|\mathbf{div}(\boldsymbol{\sigma}_h) + \varphi_h\, \boldsymbol{g}\|_{0,T}^2 \\ & + h_T^2\, \|\mathrm{curl}\big((\boldsymbol{\sigma}_h + \boldsymbol{u}_h \otimes \boldsymbol{u}_h)^{\mathtt{d}}\big)\|_{0,T}^2 + \sum_{e\in\mathcal{E}_{h,T}(\Omega)} h_e\, \|\,[\![(\boldsymbol{\sigma}_h + \boldsymbol{u}_h \otimes \boldsymbol{u}_h)^{\mathtt{d}}\, \boldsymbol{s}]\!]\|_{0,e}^2 \\ & + \sum_{e\in\mathcal{E}_{h,T}(\Gamma)} \|\boldsymbol{u}_h - \boldsymbol{u}_D\|_{0,e}^2 \,+\, h_e \Big\| (\boldsymbol{\sigma}_h \,+\, \boldsymbol{u}_h \otimes \boldsymbol{u}_h)^{\mathtt{d}} \boldsymbol{s} \,-\, \mu \frac{d\boldsymbol{u}_D}{d\boldsymbol{s}} \Big\|_{0,e}^2, \end{aligned} \tag{3.1}$$

$$\begin{aligned} \boldsymbol{\theta}_{T,\mathtt{h}}^2 \,:=\, & \|\mathbb{K}^{-1}\mathbf{p}_h \,+\, \mathbb{K}^{-1}\varphi_h\, \boldsymbol{u}_h \,-\, \nabla\varphi_h\|_{0,T}^2 \,+\, \|\mathrm{div}(\mathbf{p}_h)\|_{0,T}^2 \\ & + h_T^2\, \|\mathrm{rot}\big(\mathbb{K}^{-1}\mathbf{p}_h \,+\, \mathbb{K}^{-1}\varphi_h\, \boldsymbol{u}_h\big)\|_{0,T}^2 \,+\, \sum_{e\in\mathcal{E}_{h,T}(\Omega)} h_e\, \|\,[\![\big(\mathbb{K}^{-1}\mathbf{p}_h \,+\, \mathbb{K}^{-1}\varphi_h\, \boldsymbol{u}_h\big)\cdot \boldsymbol{s}]\!]\|_{0,e}^2 \\ & + \sum_{e\in\mathcal{E}_{h,T}(\Gamma)} \|\varphi_h - \varphi_D\|_{0,e}^2 \,+\, h_e \Big\| \big(\mathbb{K}^{-1}\mathbf{p}_h \,+\, \mathbb{K}^{-1}\varphi_h\, \boldsymbol{u}_h\big)\cdot \boldsymbol{s} \,-\, \frac{d\varphi_D}{d\boldsymbol{s}} \Big\|_{0,e}^2, \end{aligned} \tag{3.2}$$

based on which we define now the global a posteriori error estimator:

$$\boldsymbol{\theta} \,:=\, \Big\{ \sum_{T\in\mathcal{T}_h} \boldsymbol{\theta}_{T,\mathtt{f}}^2 \,+\, \sum_{T\in\mathcal{T}_h} \boldsymbol{\theta}_{T,\mathtt{h}}^2 \Big\}^{1/2}. \tag{3.3}$$

Observe, from the strong form of the problem (cf. (2.3)) and the regularity of the weak solution at the continuous level (cf. (2.4)), that each term defining $\boldsymbol{\theta}$ has a residual character, and differently from the corresponding one derived for our mixed–primal approach in [10], this is fully-local and computable; an advantageous feature for practical purposes in order to define and validate the performance of the associated adaptive algorithm.

Let us now introduce the main result of this work.

Theorem 3.1 *Let $(\boldsymbol{\sigma}, \boldsymbol{u}, \mathbf{p}, \varphi)$ and $(\boldsymbol{\sigma}_h, \boldsymbol{u}_h, \mathbf{p}_h, \varphi_h)$ be the unique solutions to problems (2.4) and (2.19) and further assume that the Dirichlet data $\boldsymbol{u}_D$ and φ_D are piecewise polynomials in $\mathbf{H}^1(\Gamma)$ and $\mathrm{H}^1(\Gamma)$, respectively. Then, there exist positive constants $C_{\mathrm{rel}}, C_{\mathrm{eff}} > 0$, depending on physical and stabilization parameters, but independent of h, such that*

$$C_{\mathrm{eff}}\, \boldsymbol{\theta} \,\leq\, \|(\boldsymbol{\sigma}, \boldsymbol{u}, \mathbf{p}, \varphi) \,-\, (\boldsymbol{\sigma}_h, \boldsymbol{u}_h, \mathbf{p}_h, \varphi_h)\| \,\leq\, C_{\mathrm{rel}}\, \boldsymbol{\theta}\,, \tag{3.4}$$

provided the data is sufficiently small (cf. Lemma 3.3).

In this result, the requirement on $\boldsymbol{u}_D$ and φ_D to be piecewise polynomials is only to show the lower bound of the estimator $\boldsymbol{\theta}$ (cf. Lemma 3.15 in [10] and Lemma 3.11 below), and is a technical assumption just to simplify the presentation. However, this can be relaxed by assuming that they are sufficiently smooth on Γ. By doing so one could use suitable polynomial approximations to derive the lower bound of $\boldsymbol{\theta}$ which would yield high–order terms.

The proof of Theorem 3.1 is carried out through Sections 3.2 and 3.3. There, we show separately that the estimator $\boldsymbol{\theta}$ satisfies the upper (reliability property) and lower (efficiency property) bounds of the expression (3.4).

3.2 Reliability of the estimator

3.2.1 Preliminary error estimates

We begin the derivation of the upper bound of (3.4) by recalling that, since $\|\boldsymbol{u}\|_{1,\Omega} \leq r$ by Theorem 2.1, the bilinear form $\mathbf{A} + \mathbf{B}_{\boldsymbol{u}}$ is elliptic on $\mathbb{H}_0(\mathbf{div};\Omega) \times \mathbf{H}^1(\Omega)$ with ellipticity constant $\alpha(\Omega)/2$ (see [11, Section 3.3]). Then, proceeding analogously to the proof of [10, Lemma 3.2], that is by using a global inf-sup condition, we obtain that there exists $C > 0$, independent of h, such that

$$\begin{aligned} \|(\boldsymbol{\sigma},\boldsymbol{u}) - (\boldsymbol{\sigma}_h,\boldsymbol{u}_h)\| \leq C \Big\{ & \|\mu\nabla\boldsymbol{u}_h - (\boldsymbol{u}_h\otimes\boldsymbol{u}_h)^{\mathtt{d}} - \boldsymbol{\sigma}_h^{\mathtt{d}}\|_{0,\Omega} + \|\mathbf{div}(\boldsymbol{\sigma}_h) + \varphi_h\,\boldsymbol{g}\|_{0,\Omega} \\ & + \|\boldsymbol{u}_h - \boldsymbol{u}_D\|_{0,\Gamma} + \|\boldsymbol{g}\|_{\infty,\Omega}\,\|\varphi-\varphi_h\|_{1,\Omega} + \|\boldsymbol{u}_h\|_{1,\Omega}\,\|\boldsymbol{u}-\boldsymbol{u}_h\|_{1,\Omega} + \big\|\mathcal{R}^{\mathtt{f}}\big\| \Big\}, \end{aligned} \tag{3.5}$$

where $\mathcal{R}^{\mathtt{f}} : \mathbb{H}_0(\mathbf{div};\Omega) \longrightarrow \mathrm{R}$ is the functional defined as

$$\mathcal{R}^{\mathtt{f}}(\boldsymbol{\tau}) = F_{\varphi_h}(\boldsymbol{\tau},\mathbf{0}) + F_D(\boldsymbol{\tau},\mathbf{0}) - \mathbf{A}(\,(\boldsymbol{\sigma}_h,\boldsymbol{u}_h)\,,\,(\boldsymbol{\tau},\mathbf{0})\,) - \mathbf{B}_{\boldsymbol{u}_h}(\,(\boldsymbol{\sigma}_h,\boldsymbol{u}_h)\,,\,(\boldsymbol{\tau},\mathbf{0})\,) \tag{3.6}$$

and $\mathbf{A}$, $\mathbf{B}_{\boldsymbol{u}_h}$, F_{φ_h} and F_D are the forms given by (2.5)-(2.6) and (2.9)-(2.10).

Next we derive an analogous preliminary bound for the error associated to the heat variables.

Lemma 3.2 *There exists a positive constant $C > 0$, independent of h, such that*

$$\begin{aligned} \|(\mathbf{p},\varphi) - (\mathbf{p}_h,\varphi_h)\| \leq C \Big\{ & \|\mathbb{K}^{-1}\mathbf{p}_h + \mathbb{K}^{-1}\varphi_h\,\boldsymbol{u}_h - \nabla\varphi_h\|_{0,\Omega} + \|\mathrm{div}(\mathbf{p}_h)\|_{0,\Omega} \\ & + \|\varphi_h - \varphi_D\|_{0,\Gamma} + \|\mathbb{K}^{-1}\|_{\infty,\Omega}\,\|\varphi-\varphi_h\|_{1,\Omega} + \|\varphi\|_{1,\Omega}\,\|\boldsymbol{u}-\boldsymbol{u}_h\|_{1,\Omega} + \big\|\mathcal{R}^{\mathtt{h}}\big\| \Big\}, \end{aligned} \tag{3.7}$$

where $\mathcal{R}^{\mathtt{h}} : \mathbf{H}(\mathrm{div};\Omega) \longrightarrow \mathrm{R}$ is the functional defined as

$$\mathcal{R}^{\mathtt{h}}(\mathbf{q}) = \widetilde{F}_D(\mathbf{q},0) - \widetilde{\mathbf{A}}(\,(\mathbf{p}_h,\varphi_h)\,,\,(\mathbf{q},0)\,) - \widetilde{\mathbf{B}}_{\boldsymbol{u}_h}(\,(\mathbf{p}_h,\varphi_h)\,,\,(\mathbf{q},\mathbf{0})\,), \tag{3.8}$$

and $\widetilde{\mathbf{A}}$, $\widetilde{\mathbf{B}}_{\boldsymbol{u}_h}$, and $\widetilde{F}_D$ are the forms given by (2.7)-(2.8) and (2.11).

Proof. According to [11, Lemma 3.3] and the fact that $\|\boldsymbol{u}\|_{1,\Omega} \leq r$, we have that the bilinear form $\widetilde{\mathbf{A}} + \widetilde{\mathbf{B}}_{\boldsymbol{u}}$ is uniformly elliptic on $\mathbf{H}(\mathrm{div};\Omega) \times \mathrm{H}^1(\Omega)$ with a positive constant $\widetilde{\alpha}(\Omega)/2$, independent of $\boldsymbol{u}$. This implies that

$$\begin{aligned} \frac{\widetilde{\alpha}(\Omega)}{2}\|(\mathbf{p},\varphi) - (\mathbf{p}_h,\varphi_h)\| &\leq \sup_{\substack{(\mathbf{q},\psi)\in\mathbf{H}(\mathrm{div};\Omega)\times\mathrm{H}^1(\Omega)\\(\mathbf{q},\psi)\neq\mathbf{0}}} \frac{\big(\widetilde{\mathbf{A}}+\widetilde{\mathbf{B}}_{\boldsymbol{u}}\big)(\,(\mathbf{p},\varphi) - (\mathbf{p}_h,\varphi_h)\,,\,(\mathbf{q},\psi)\,)}{\|(\mathbf{q},\psi)\|} \\ &= \sup_{\substack{(\mathbf{q},\psi)\in\mathbf{H}(\mathbf{div};\Omega)\times\mathbf{H}^1(\Omega)\\(\mathbf{q},\psi)\neq\mathbf{0}}} \frac{\widetilde{F}_D(\mathbf{q},\psi) - \big(\widetilde{\mathbf{A}}+\widetilde{\mathbf{B}}_{\boldsymbol{u}_h}\big)((\mathbf{p}_h,\varphi_h),(\mathbf{q},\psi)) - \widetilde{\mathbf{B}}_{\boldsymbol{u}-\boldsymbol{u}_h}((\mathbf{p}_h,\varphi_h),(\mathbf{q},\psi))}{\|(\mathbf{q},\psi)\|}. \end{aligned} \tag{3.9}$$

Then, manipulating terms and using the Cauchy-Schwarz and Hölder's inequalities, we find that

$$\begin{aligned}
&\widetilde{F}_D(\mathbf{q},\psi) - \big(\widetilde{\mathbf{A}} + \widetilde{\mathbf{B}}_{\boldsymbol{u}_h}\big)\big(\,(\mathbf{p}_h,\varphi_h)\,,\,(\mathbf{q},\psi)\,\big) - \widetilde{\mathbf{B}}_{\boldsymbol{u}-\boldsymbol{u}_h}\big(\,(\mathbf{p}_h,\varphi_h)\,,\,(\mathbf{q},\psi)\,\big) \\
&\quad \leq \Big\{ \kappa_4 \,\|\mathbb{K}^{-1}\mathbf{p}_h + \mathbb{K}^{-1}\varphi_h\,\boldsymbol{u}_h - \nabla\varphi_h\|_{0,\Omega} + \|\mathrm{div}(\mathbf{p}_h)\|_{0,\Omega} + \kappa_6\,\|\varphi_h - \varphi_D\|_{0,\Gamma}\Big\}\,\|\psi\|_{1,\Omega} \\
&\quad + \quad \|\mathbb{K}^{-1}\|_{\infty,\Omega}\,\|\varphi_h\|_{1,\Omega}\,\|\boldsymbol{u}-\boldsymbol{u}_h\|_{1,\Omega}\,\|(\mathbf{q},\psi)\| + \mathcal{R}^{\mathtt{h}}(\mathbf{q})\,.
\end{aligned}$$

Next, by adding and substracting φ in the norm $\|\varphi_h\|_{1,\Omega}$ appearing in the last row, using that $\|\boldsymbol{u}\|_{1,\Omega}$ and $\|\boldsymbol{u}_h\|_{1,\Omega}$ are upperly bounded by r, replacing then back in (3.9), and simplifying the resulting expression, we easily obtain (3.7) with a constant $C > 0$ depending only on r and the stabilization parameters $\kappa_i\,(i = 4, 6)$. □

As a straightforward consequence of the foregoing analysis we derive now a preliminary upper bound for the total error.

Lemma 3.3 *Assume that the data is sufficiently small so that the constant $C(\boldsymbol{g},\mathbb{K}^{-1},\boldsymbol{u}_D,\varphi_D)$, defined below in (3.12) is such that $C(\boldsymbol{g},\mathbb{K}^{-1},\boldsymbol{u}_D,\varphi_D) \leq 1/2$. Then, the total error satisfies*

$$\begin{aligned}
&\|(\boldsymbol{\sigma},\boldsymbol{u},\mathbf{p},\varphi) - (\boldsymbol{\sigma}_h,\boldsymbol{u}_h,\mathbf{p}_h,\varphi_h)\| \\
&\quad \leq \quad C\,\Big\{\|\mu\,\nabla\boldsymbol{u}_h - (\boldsymbol{u}_h\otimes\boldsymbol{u}_h)^{\mathtt{d}} - \boldsymbol{\sigma}_h^{\mathtt{d}}\|_{0,\Omega} + \|\mathbf{div}(\boldsymbol{\sigma}_h) + \varphi_h\boldsymbol{g}\|_{0,\Omega} + \|\boldsymbol{u}_h - \boldsymbol{u}_D\|_{0,\Gamma} \\
&\quad + \quad \|\mathbb{K}^{-1}\mathbf{p}_h + \mathbb{K}^{-1}\varphi_h\boldsymbol{u}_h - \nabla\varphi_h\|_{0,\Omega} + \|\mathrm{div}(\mathbf{p}_h)\|_{0,\Omega} + \|\varphi_h - \varphi_D\|_{0,\Gamma} \\
&\quad + \quad \big\|\mathcal{R}^{\mathtt{f}}\big\| + \big\|\mathcal{R}^{\mathtt{h}}\big\|\Big\}\,.
\end{aligned} \tag{3.10}$$

where C depends on data and stabilization parameters but is independent of h, and $\mathcal{R}^{\mathtt{f}}$ and $\mathcal{R}^{\mathtt{h}}$ are the linear functionals defined by (3.6) and (3.8), respectively.

Proof. Combining the estimates (3.5) and (3.7), we get

$$\begin{aligned}
&\|(\boldsymbol{\sigma},\boldsymbol{u},\mathbf{p},\varphi) - (\boldsymbol{\sigma}_h,\boldsymbol{u}_h,\mathbf{p}_h,\varphi_h)\| \\
&\quad \leq \quad C\,\Big\{\Big(\|\boldsymbol{g}\|_{\infty,\Omega} + \|\boldsymbol{u}_h\|_{1,\Omega} + \|\mathbb{K}^{-1}\|_{\infty,\Omega} + \|\varphi\|_{1,\Omega}\Big)\|(\boldsymbol{u},\varphi) - (\boldsymbol{u}_h,\varphi_h)\| \\
&\quad + \quad \|\mu\,\nabla\boldsymbol{u}_h - (\boldsymbol{u}_h\otimes\boldsymbol{u}_h)^{\mathtt{d}} - \boldsymbol{\sigma}_h^{\mathtt{d}}\|_{0,\Omega} + \|\mathbf{div}(\boldsymbol{\sigma}_h) + \varphi_h\boldsymbol{g}\|_{0,\Omega} + \|\boldsymbol{u}_h - \boldsymbol{u}_D\|_{0,\Gamma} \\
&\quad + \quad \|\mathbb{K}^{-1}\mathbf{p}_h + \mathbb{K}^{-1}\varphi_h\boldsymbol{u}_h - \nabla\varphi_h\|_{0,\Omega} + \|\mathbf{div}(\mathbf{p}_h)\|_{0,\Omega} + \|\varphi_h - \varphi_D\|_{0,\Gamma} \\
&\quad + \quad \big\|\mathcal{R}^{\mathtt{f}}\big\| + \big\|\mathcal{R}^{\mathtt{h}}\big\|\Big\}\,.
\end{aligned} \tag{3.11}$$

Then, using the a priori estimates for $\boldsymbol{u}_h$ and φ provided by Theorems 2.1 and 2.2, the factor multiplying $\|(\boldsymbol{u},\varphi) - (\boldsymbol{u}_h,\varphi_h)\|$ on the right-hand side of the above inequality can be bounded by

$$\begin{aligned}
C(\boldsymbol{g},\mathbb{K}^{-1},\boldsymbol{u}_D,\varphi_D) \,:=\, &\|\boldsymbol{g}\|_{\infty,\Omega} + c_{\mathbf{S}}\,\Big\{r\|\boldsymbol{g}\|_{\infty,\Omega} + \|\boldsymbol{u}_D\|_{0,\Gamma} + \|\boldsymbol{u}_D\|_{1/2,\Gamma}\Big\} \\
&+ \quad \|\mathbb{K}^{-1}\|_{\infty,\Omega} + c_{\widetilde{\mathbf{S}}}\,\Big\{\|\varphi_D\|_{0,\Gamma} + \|\varphi_D\|_{1/2,\Gamma}\Big\}\,.
\end{aligned} \tag{3.12}$$

Finally, (3.11) and the assumption on $C(\boldsymbol{g},\mathbb{K}^{-1},\boldsymbol{u}_D,\varphi_D)$ imply (3.10), which completes the proof. □

3.2.2 Estimation of the dual norms

Based on standard arguments used in duality techniques for a posteriori error analyses of mixed finite element schemes [5, 10, 20, 21, 22, 24, 25], in this Section we estimate $\mathcal{R}^{\mathtt{h}}$ and $\mathcal{R}^{\mathtt{f}}$ in their respective norms. We begin with the upper bound for $\mathcal{R}^{\mathtt{f}}$ whose proof can be found in [10, Lemma 3.11].

Lemma 3.4 *Assume that $\boldsymbol{u}_D \in \mathbf{H}^1(\Gamma)$. Then, there exists a positive constant $C > 0$, independent of h, such that*

$$\begin{aligned}\|\mathcal{R}^{\mathtt{f}}\| \leq C \Big\{ & \sum_{T\in\mathcal{T}_h} h_T^2 \, \|\mu\, \nabla \boldsymbol{u}_h - \boldsymbol{\sigma}_h^{\mathtt{d}} - (\boldsymbol{u}_h \otimes \boldsymbol{u}_h)^{\mathtt{d}}\|_{0,T}^2 + \kappa_2^2 \, \|\mathbf{div}\, \boldsymbol{\sigma}_h + \varphi_h\, \boldsymbol{g}\|_{0,T}^2 \\ & h_T^2 \, \|\mathrm{curl}\big((\boldsymbol{\sigma}_h + \boldsymbol{u}_h \otimes \boldsymbol{u}_h)^{\mathtt{d}}\big)\|_{0,T}^2 + \sum_{e\in\mathcal{E}_h(\Omega)} h_e \, \|[\![(\boldsymbol{\sigma}_h + \boldsymbol{u}_h \otimes \boldsymbol{u}_h)^{\mathtt{d}}\, \boldsymbol{s})]\!]\|_{0,e}^2 \\ & + \sum_{e\in\mathcal{E}_h(\Gamma)} h_e \Big\{ \Big\| (\boldsymbol{\sigma}_h + \boldsymbol{u}_h \otimes \boldsymbol{u}_h)^{\mathtt{d}}\, \boldsymbol{s} - \mu \frac{d\boldsymbol{u}_D}{d\boldsymbol{s}} \Big\|_{0,e}^2 + \|\boldsymbol{u} - \boldsymbol{u}_D\|_{0,e}^2 \Big\} \Big\}^{1/2} . \end{aligned} \tag{3.13}$$

We now turn to the derivation of the corresponding estimate for $\mathcal{R}^{\mathtt{h}}$. To that end we first introduce some definitions and recall some standard results.

Let $\Pi_h^k : \mathbf{H}^1(\Omega) \longrightarrow \mathbf{RT}_k(\mathcal{T}_h)$ be the usual Raviart–Thomas interpolation operator. It is well known that this operator satisfies the following approximation properties (see, [7, Section III.3.3], [18, Section 3.4.4] and [28, Lemma 1.130], for instance):

- For each $\zeta \in \mathbf{H}^m(\Omega)$, with $1 \leq m \leq k+1$,

$$\|\zeta - \Pi_h^k(\zeta)\|_{0,T} \leq C\, h_T^m \, |\zeta|_{m,T} \quad \forall\, T \in \mathcal{T}_h \,. \tag{3.14}$$

- For each $\zeta \in \mathbf{H}^1(\Omega)$ such that $\mathrm{div}(\zeta) \in \mathbf{H}^m(\Omega)$, with $0 \leq m \leq k+1$,

$$\|\mathrm{div}(\zeta - \Pi_h^k(\zeta))\|_{0,T} \leq C\, h_T^m \, |\mathrm{div}\, \zeta|_{m,T} \quad \forall\, T \in \mathcal{T}_h \,. \tag{3.15}$$

- For each $\zeta \in \mathbf{H}^1(\Omega)$, there holds

$$\|\zeta\cdot\boldsymbol{\nu} - \Pi_h^k(\zeta)\cdot\boldsymbol{\nu}\|_{0,e} \leq C\, h_e^{1/2} \, |\zeta|_{1,T_e} \,, \tag{3.16}$$

  where T_e is the element of $\mathcal{T}_h$ having e as an edge.

In turn, we consider the space $\mathrm{X}_h = \Big\{ v_h \in \mathrm{C}(\bar\Omega) : \quad v_h\big|_T \in \mathrm{P}_1(T) \quad \forall\, T \in \mathcal{T}_h \Big\}$ and denote by $I_h : \mathrm{H}^1(\Omega) \longrightarrow \mathrm{X}_h$ the Clément interpolation operator. From this operator we will only utilize the following local estimates (see [9]): For each $v \in \mathrm{H}^1(\Omega)$ there hold

$$\|v - I_h v\|_{0,T} \leq C\, h_T \, |v|_{1,\Delta(T)} \quad \forall\, T \in \mathcal{T}_h \,, \quad \text{and} \quad \|v - I_h v\|_{0,e} \leq C\, h_e^{1/2} \, \|v\|_{1,\Delta(e)} \quad \forall\, e \in \mathcal{E}_h \,, \tag{3.17}$$

where $\Delta(T)$ and $\Delta(e)$ are the unions of all elements intersecting T and e, respectively.

Finally we recall from [14, Lemma 3.4] the following result which provides the last ingredient we need: a stable Helmholtz decomposition of the space $\mathbf{H}(\mathrm{div};\Omega)$.

Lemma 3.5 *For each $\mathbf{q} \in \mathbf{H}(\mathrm{div};\Omega)$ there exist $z \in \mathrm{H}^2(\Omega)$ and $\phi \in \mathrm{H}^1(\Omega)$, such that*

$$\mathbf{q} = \nabla z + \mathbf{curl}(\phi) \quad \textit{in} \quad \Omega \,, \quad \textit{and} \quad \|z\|_{2,\Omega} + \|\phi\|_{1,\Omega} \leq C\, \|\mathbf{q}\|_{\mathrm{div},\Omega} \,. \tag{3.18}$$

To start the derivation of the upper bound of $\mathcal{R}^{\mathtt{h}}$ we first notice, according to its own definition, that there holds

$$\mathcal{R}^{\mathtt{h}}(\mathbf{q}_h) = 0 \qquad \forall\, \mathbf{q}_h \in \mathbf{H}^{\mathbf{p}}_h.$$

In turn, given $\mathbf{q} \in \mathbf{H}(\mathrm{div};\Omega)$ and provided its Helmholtz decomposition $\mathbf{q} = \nabla z + \mathbf{curl}(\phi)$ with $z \in \mathrm{H}^2(\Omega)$ and $\phi \in \mathrm{H}^1(\Omega)$, we let

$$\mathbf{q}_h := \Pi^k_h(\nabla z) + \mathbf{curl}(I_h\phi) \in \mathbf{H}^{\mathbf{p}}_h\,.$$

Then, using that $\langle\, \nabla z\cdot\boldsymbol{\nu}\,, \varphi_h\,\rangle_\Gamma = \int_\Omega \varphi_h\,\mathrm{div}(\nabla z) + \int_\Omega \nabla\varphi_h\cdot\nabla z$, and performing simple computations, it is not difficult to see that

$$\mathcal{R}^{\mathtt{h}}(\mathbf{q}) = \mathcal{R}^{\mathtt{h}}(\mathbf{q}-\mathbf{q}_h) = \mathcal{R}^{\mathtt{h}}(\nabla z - \Pi^k_h(\nabla z)) + \mathcal{R}^{\mathtt{h}}(\mathbf{curl}(\phi - I_h\phi))\,, \tag{3.19}$$

where

$$\begin{aligned}\mathcal{R}^{\mathtt{h}}(\nabla z - \Pi^k_h(\nabla z)) &= \int_\Omega \big(\nabla\varphi_h - \mathbb{K}^{-1}\mathbf{p}_h - \mathbb{K}^{-1}\varphi_h\boldsymbol{u}_h\big)\cdot(\nabla z - \Pi^k_h(\nabla z))\\ &\quad - \kappa_5\int_\Omega \mathrm{div}(\mathbf{p}_h)\,\mathrm{div}(\nabla z - \Pi^k_h(\nabla z)) + \langle\, \nabla z\cdot\boldsymbol{\nu} - \Pi^k_h(\nabla z)\cdot\boldsymbol{\nu}, \varphi_D - \varphi_h\,\rangle_\Gamma\end{aligned} \tag{3.20}$$

and

$$\mathcal{R}^{\mathtt{h}}(\mathbf{curl}(\phi - I_h\phi)) := -\int_\Omega \big(\mathbb{K}^{-1}\mathbf{p}_h - \mathbb{K}^{-1}\varphi_h\boldsymbol{u}_h\big)\cdot\mathbf{curl}(\phi - I_h\phi) + \langle\, \mathbf{curl}(\phi - I_h\phi)\cdot\boldsymbol{\nu}\,, \varphi_D\,\rangle_\Gamma\,. \tag{3.21}$$

In this way, to derive the desired estimate for $\mathcal{R}^{\mathtt{h}}$, in what follows we make use of the approximation properties of Π^k_h and I_h and estimates (3.20) and (3.21). We begin with the upper bound of (3.20).

Lemma 3.6 *There exists a positive constant C, independent of h, such that*

$$\begin{aligned}\mathcal{R}^{\mathtt{h}}(\nabla z - \Pi^k_h(\nabla z)) \le C\Bigg\{ &\sum_{T\in\mathcal{T}_h} h_T^2\,\|\nabla\varphi_h - \mathbb{K}^{-1}\mathbf{p}_h - \mathbb{K}^{-1}\varphi_h\boldsymbol{u}_h\|^2_{0,T}\\ &+ \sum_{T\in\mathcal{T}_h}\kappa_5^2\,\|\mathrm{div}(\mathbf{p}_h)\|^2_{0,T} + \sum_{e\in\mathcal{E}_h(\Gamma)} h_e\|\varphi_D - \varphi_h\|^2_{0,e}\Bigg\}^{1/2}\|\mathbf{q}\|_{\mathrm{div},\Omega}.\end{aligned} \tag{3.22}$$

Proof. On the one hand, combining the Cauchy-Schwarz inequality and the property (3.14) with $m = 1$ we get

$$\Big|\int_T \big(\nabla\varphi_h - \mathbb{K}^{-1}\mathbf{p}_h - \mathbb{K}^{-1}\varphi_h\boldsymbol{u}_h\big)\cdot(\nabla z - \Pi^k_h(\nabla z))\Big| \le h_T\big\|\nabla\varphi_h - \mathbb{K}^{-1}\mathbf{p}_h - \mathbb{K}^{-1}\varphi_h\boldsymbol{u}_h\big\|_{0,T}|\nabla z|_{1,T}\,.$$

On the other hand, employing the approximation property (3.15) with $m = 0$, and using next that $\mathrm{div}(\nabla z) = \mathrm{div}(\mathbf{q})$, we also find that

$$\Big|\kappa_5\int_T \mathrm{div}(\mathbf{p}_h)\,\mathrm{div}(\nabla z - \Pi^k_h(\nabla z))\Big| \le C\,\kappa_5\,\|\mathrm{div}(\mathbf{p}_h)\|_{0,T}\|\mathrm{div}(\mathbf{q})\|_{0,T}\,.$$

The property (3.16) allows us to state that

$$\Big|\langle\, \nabla z\cdot\boldsymbol{\nu} - \Pi^k_h(\nabla z)\cdot\boldsymbol{\nu}, \varphi_D - \varphi_h\,\rangle_\Gamma\Big| \le C\Bigg\{\sum_{e\in\mathcal{E}_h(\Gamma)} h_e\|\varphi_D - \varphi_h\|^2_{0,e}\Bigg\}^{1/2}|\nabla z|_{1,\Omega}$$

Then, from the regularity of the mesh, the estimate (3.22) follows as a direct consequence of (3.18) and the Cauchy-Schwarz inequality. □

The following lemma establishes the upper bound for (3.21).

Lemma 3.7 *Assume that $\varphi_D \in \mathrm{H}^1(\Gamma)$. Then, there exists a positive constant $C > 0$, independent of h, such that*

$$\begin{aligned}\mathcal{R}^{\mathtt{h}}(\mathbf{curl}(\phi - I_h\phi)) \,\leq\, C \Big\{ & \sum_{T\in\mathcal{T}_h} h_T^2 \,\|\mathrm{rot}\big(\mathbb{K}^{-1}\mathbf{p}_h - \mathbb{K}^{-1}\varphi_h\boldsymbol{u}_h\big)\|_{0,T}^2 \\ & + \sum_{e\in\mathcal{E}_h(\Omega)} h_e \|\,[\![\big(\mathbb{K}^{-1}\mathbf{p}_h - \mathbb{K}^{-1}\varphi_h\boldsymbol{u}_h\big)\cdot\boldsymbol{s}]\!]\|_{0,e}^2 \\ & + \sum_{e\in\mathcal{E}_h(\Gamma)} h_e \Big\| \big(\mathbb{K}^{-1}\mathbf{p}_h - \mathbb{K}^{-1}\varphi_h\boldsymbol{u}_h\big)\cdot\boldsymbol{s} - \frac{d\varphi_D}{d\boldsymbol{s}}\Big\|_{0,e}^2 \Big\}^{1/2} \|\mathbf{q}\|_{\mathrm{div},\Omega}.\end{aligned} \tag{3.23}$$

Proof. Similarly to [14, Lemma 3.10] we integrate by parts on each element and on the boundary (the latter requires that $\varphi_D \in \mathrm{H}^1(\Gamma)$), and apply estimates (3.17), to find that

$$\begin{aligned}\mathcal{R}^{\mathtt{h}}(\mathbf{curl}(\phi - I_h\phi)) &= -\sum_{T\in\mathcal{T}_h}\int_T \big(\mathbb{K}^{-1}\mathbf{p}_h - \mathbb{K}^{-1}\varphi_h\boldsymbol{u}_h\big)\cdot\mathbf{curl}(\phi - I_h\phi) \\ &+ \quad \langle \mathbf{curl}(\phi - I_h\phi)\cdot\boldsymbol{\nu}\,, \varphi_D\,\rangle_\Gamma \\ &= -\sum_{T\in\mathcal{T}_h}\int_T \mathrm{rot}\big(\mathbb{K}^{-1}\mathbf{p}_h - \mathbb{K}^{-1}\varphi_h\boldsymbol{u}_h\big)\,(\phi - I_h\phi) \\ &+ \quad \sum_{e\in\mathcal{E}_h(\Omega)}\int_e [\![\big(\mathbb{K}^{-1}\mathbf{p}_h - \mathbb{K}^{-1}\varphi_h\boldsymbol{u}_h\big)\cdot\boldsymbol{s}]\!](\phi - I_h\phi) \\ &+ \quad \sum_{e\in\mathcal{E}_h(\Gamma)}\int_e \Big\{\,\big(\mathbb{K}^{-1}\mathbf{p}_h - \mathbb{K}^{-1}\varphi_h\boldsymbol{u}_h\big)\cdot\boldsymbol{s} \,-\, \frac{d\varphi_D}{d\boldsymbol{s}}\,\Big\}\,(\phi - I_h\phi) \\ &\leq C\Big\{ \sum_{T\in\mathcal{T}_h} h_T \|\mathrm{rot}\big(\mathbb{K}^{-1}\mathbf{p}_h - \mathbb{K}^{-1}\varphi_h\boldsymbol{u}_h\big)\|_{0,T}\|\phi\|_{1,\Delta(T)} \\ &+ \quad \Big(\sum_{e\in\mathcal{E}_h(\Omega)} h_e^{1/2} \|\,[\![\big(\mathbb{K}^{-1}\mathbf{p}_h - \mathbb{K}^{-1}\varphi_h\boldsymbol{u}_h\big)\cdot\boldsymbol{s}]\!]\|_{0,e} \\ &+ \quad \sum_{e\in\mathcal{E}_h(\Gamma)} h_e^{1/2} \Big\| \big(\mathbb{K}^{-1}\mathbf{p}_h - \mathbb{K}^{-1}\varphi_h\boldsymbol{u}_h\big)\cdot\boldsymbol{s} \,-\, \frac{d\varphi_D}{d\boldsymbol{s}}\Big\|_{0,e}\Big)\,\|\phi\|_{1,\Delta(e)}\Big\}.\end{aligned}$$

Then, using again the bound in (3.18), the fact that the number of triangles in $\Delta(T)$ and $\Delta(e)$ are bounded, and applying the Cauchy–Schwarz inequality we easily obtain (3.23). □

We are now in position of establishing the upper bound for $\mathcal{R}^{\mathtt{h}}$.

Lemma 3.8 *There exists a positive constant $C > 0$, independent of h, such that*

$$\begin{aligned}\|\mathcal{R}^{\mathtt{h}}\| \,\leq\, C\Big\{ & \sum_{T\in\mathcal{T}_h} h_T^2 \,\|\nabla\varphi_h - \mathbb{K}^{-1}\mathbf{p}_h - \mathbb{K}^{-1}\varphi_h\boldsymbol{u}_h\|_{0,T}^2 \,+\, \kappa_5^2\,\|\mathrm{div}(\mathbf{p}_h)\|_{0,T}^2 \\ & + h_T^2\,\|\mathrm{rot}\big(\mathbb{K}^{-1}\mathbf{p}_h - \mathbb{K}^{-1}\varphi_h\boldsymbol{u}_h\big)\|_{0,T}^2 \,+\, \sum_{e\in\mathcal{E}_h(\Omega)} h_e\,\|\,[\![\big(\mathbb{K}^{-1}\mathbf{p}_h - \mathbb{K}^{-1}\varphi_h\boldsymbol{u}_h\big)\cdot\boldsymbol{s}]\!]\|_{0,e}^2 \\ & + \sum_{e\in\mathcal{E}_h(\Gamma)} h_e\Big(\Big\| \big(\mathbb{K}^{-1}\mathbf{p}_h - \mathbb{K}^{-1}\varphi_h\boldsymbol{u}_h\big)\cdot\boldsymbol{s} \,-\, \frac{d\varphi_D}{d\boldsymbol{s}}\Big\|_{0,e}^2 \,+\, \|\varphi_h - \varphi_D\|_{0,e}^2\Big)\Big\}^{1/2}.\end{aligned} \tag{3.24}$$

Proof. It suffices to use the identity (3.19) and estimates (3.22) and (3.23). □

To close this section, we note that the terms $h_T^2 \, \|\mu \, \nabla \boldsymbol{u}_h - \boldsymbol{\sigma}_h^{\mathtt{d}} - (\boldsymbol{u}_h \otimes \boldsymbol{u}_h)^{\mathtt{d}}\|_{0,T}$, $h_T^2 \, \|\nabla \varphi_h - \mathbb{K}^{-1} \mathbf{p}_h - \mathbb{K}^{-1} \varphi_h \boldsymbol{u}_h\|_{0,T}$, $h_e \, \|\boldsymbol{u}_h - \boldsymbol{u}_D\|_{0,T}$ and $h_e \, \|\varphi_h - \varphi_D\|_{0,T}$, appearing in the estimates (3.13) and (3.24) are clearly dominated by $\|\mu \, \nabla \boldsymbol{u}_h - \boldsymbol{\sigma}_h^{\mathtt{d}} - (\boldsymbol{u}_h \otimes \boldsymbol{u}_h)^{\mathtt{d}}\|_{0,T}$, $\|\nabla \varphi_h - \mathbb{K}^{-1} \mathbf{p}_h - \mathbb{K}^{-1} \varphi_h \boldsymbol{u}_h\|_{0,T}$, $\|\boldsymbol{u}_h - \boldsymbol{u}_D\|_{0,T}$ and $\|\varphi_h - \varphi_D\|_{0,T}$, respectively, already appearing in the first total preliminary estimate provided by Lemma 3.3. As a result, the reliability property of $\boldsymbol{\theta}$ (cf. upper bound in Theorem 3.1) is deduced from this fact and a combination of Lemmas 3.3, 3.4 and 3.8, and the resulting multiplicative constant, denoted by C_{rel}, is clearly independent of h.

3.3 Efficiency

In this section we focus on showing the lower bound in (3.4). To do so, we firstly note that the estimator $\boldsymbol{\theta}_{T,\mathtt{f}}$ (cf. (3.1)) associated to the fluid equations retains the same structure of the corresponding one in our adaptive mixed–primal method [10], from where we immediately deduce its efficiency property and state it through the next result as follows.

Lemma 3.9 *Let $(\boldsymbol{\sigma}, \boldsymbol{u}, \varphi)$ and $(\boldsymbol{\sigma}_h, \boldsymbol{u}_h, \varphi_h)$ be the unique solutions to problems (2.4) and (2.19), respectively, and assume that the trace $\boldsymbol{u}_D$ is a piecewise polynomial in $\mathbf{H}^1(\Gamma)$. Then, there exists a positive constant C, depending on physical constants and on the stabilization parameters, but independent of h, such that*

$$C \left\{ \sum_{T \in \mathcal{T}_h} \boldsymbol{\theta}_{T,\mathtt{f}}^2 \right\}^{1/2} \leq \|(\boldsymbol{\sigma}, \boldsymbol{u}, \varphi) - (\boldsymbol{\sigma}_h, \boldsymbol{u}_h, \varphi_h)\| \, .$$

Proof. It essentially follows by combining Lemmas 3.14 and 3.15 in [10, Section 3.3]. □

Next, to state an analogous estimate for the terms involved in the indicator $\boldsymbol{\theta}_{T,\mathtt{h}}$ (cf. (3.2)), we make extensive use of the original system of equations (2.3), which is recovered from the augmented continuous formulation (2.4) by choosing suitable test functions and integrating by parts backwardly the corresponding equations. We begin with the estimates for the zero order terms appearing in the definition of $\boldsymbol{\theta}_{T,\mathtt{h}}$.

Lemma 3.10 *There holds*

$$\|\mathrm{div}(\mathbf{p}) - \mathrm{div}(\mathbf{p}_h)\|_{0,T} \leq \|\mathbf{p} - \mathbf{p}_h\|_{\mathrm{div},T} \qquad \forall \, T \in \mathcal{T}_h.$$

Moreover, there exist C_1, $C_2 > 0$, independent of h, such that

$$\sum_{T \in \mathcal{T}_h} \|\mathbb{K}^{-1} \, \mathbf{p}_h + \mathbb{K}^{-1} \, \varphi_h \, \boldsymbol{u}_h - \nabla \varphi_h\|_{0,T}^2 \leq C_1 \, \|(\boldsymbol{u}, \mathbf{p}, \varphi) - (\boldsymbol{u}_h, \mathbf{p}_h, \varphi_h)\|^2$$

and

$$\sum_{e \in \mathcal{E}_h(\Gamma)} \|\varphi_h - \varphi_D\|_{0,e}^2 \leq C_2 \, \|\varphi - \varphi_h\|_{1,\Omega}^2 \, .$$

Proof. First, since $\mathrm{div}(\mathbf{p}) = 0$ in Ω, it readily follows that

$$\|\mathrm{div}(\mathbf{p}_h)\|_{0,T} = \|\mathrm{div}(\mathbf{p}) - \mathrm{div}(\mathbf{p}_h)\|_{0,T} \leq \|\mathbf{p} - \mathbf{p}_h\|_{\mathrm{div},T} \, .$$

In turn, since $\varphi|_\Gamma = \varphi_D$, by the trace inequality in $\mathrm{H}^1(\Omega)$ we easily have that

$$\sum_{e \in \mathcal{E}_h(\Gamma)} \|\varphi_h - \varphi_D\|_{0,e}^2 \leq C \, \|\varphi - \varphi_h\|_{1,\Omega}^2 \, .$$

Likewise, to state the second statement we use that $\mathbb{K}^{-1}\,\mathbf{p} + \mathbb{K}^{-1}\,\varphi\,\boldsymbol{u} - \nabla\varphi = 0$ in Ω and the identity

$$\varphi\ \boldsymbol{u} - \varphi_h\ \boldsymbol{u}_h\ =\ (\boldsymbol{u}\ -\ \boldsymbol{u}_h)\,\varphi\ +\ (\varphi\ -\ \varphi_h)\,\boldsymbol{u}_h\,, \tag{3.25}$$

to deduce from the triangle inequality that

$$\begin{aligned}\|\mathbb{K}^{-1}\,\mathbf{p}_h\ +\ \mathbb{K}^{-1}\,\varphi_h\,\boldsymbol{u}_h\ -\ \nabla\varphi_h\|_{0,T}^2\ \leq\ C\,\Big\{\,&\|\mathbb{K}^{-1}\|_{\infty,\Omega}^2\|\mathbf{p}-\mathbf{p}_h\|_{0,T}^2\\ +\quad&\|\mathbb{K}^{-1}\|_{\infty,\Omega}^2\|\,(\boldsymbol{u}-\boldsymbol{u}_h)\varphi\ +\ (\varphi-\varphi_h)\,\boldsymbol{u}_h\|_{0,T}^2\ +\ \|\nabla(\varphi-\varphi_h)\|_{0,T}^2\,\Big\}\,,\end{aligned} \tag{3.26}$$

and hence, the proof concludes by adding on $T\in\mathcal{T}_h$, and using the Hölder inequality, a Sobolev embedding and the fact that $\|\boldsymbol{u}_h\|_{1,\Omega}, \|\varphi\|_{1,\Omega} \leq r$ (see Theorems 2.1 and 2.2) to bound the second term at the right-hand side of (3.26) as

$$\begin{aligned}&\sum_{T\in\mathcal{T}_h}\|(\boldsymbol{u}-\boldsymbol{u}_h)\varphi\ +\ (\varphi-\varphi_h)\,\boldsymbol{u}_h\|_{0,T}^2\\ &\qquad\leq\ \|\boldsymbol{u}-\boldsymbol{u}_h\|_{\mathbf{L}^4(\Omega)}^2\|\varphi\|_{\mathrm{L}^4(\Omega)}^2\ +\ \|\varphi-\varphi_h\|_{\mathrm{L}^4(\Omega)}^2\|\boldsymbol{u}_h\|_{\mathbf{L}^4(\Omega)}^2\\ &\qquad\leq C(r)\,\Big\{\,\|\boldsymbol{u}-\boldsymbol{u}_h\|_{1,\Omega}^2\ +\ \|\varphi-\varphi_h\|_{1,\Omega}^2\,\Big\},\end{aligned}$$

and the resulting constant C_1 depends on $\mathbb{K}$ and r but is independent on h. □

The corresponding bounds for the remaining terms defining $\boldsymbol{\theta}_{T,\mathrm{h}}$ are stated next.

Lemma 3.11 *There exist $C_3,\ C_4>0$, independent of h, such that*

$$\sum_{T\in\mathcal{T}_h} h_T^2\|\mathrm{rot}\big(\mathbb{K}^{-1}\mathbf{p}_h-\mathbb{K}^{-1}\varphi_h\boldsymbol{u}_h\big)\|_{0,T}^2\ \leq\ C_3\,\|(\boldsymbol{u},\mathbf{p},\varphi)\ -\ (\boldsymbol{u}_h,\mathbf{p}_h,\varphi_h)\|^2\,, \tag{3.27}$$

$$\sum_{e\in\mathcal{E}_h(\Omega)} h_e\|\,[\![\big(\mathbb{K}^{-1}\mathbf{p}_h-\mathbb{K}^{-1}\varphi_h\boldsymbol{u}_h\big)\cdot\boldsymbol{s}]\!]\|_{0,e}^2\ \leq\ C_4\,\|(\boldsymbol{u},\mathbf{p},\varphi)\ -\ (\boldsymbol{u}_h,\mathbf{p}_h,\varphi_h)\|^2\,. \tag{3.28}$$

In addition, if φ_D is piecewise polynomial on each $e\in\mathcal{E}_h(\Gamma)$, then there exists $C_5>0$, independent of h, such that

$$\sum_{e\in\mathcal{E}_h(\Gamma)} h_e\left\|\big(\mathbb{K}^{-1}\mathbf{p}_h-\mathbb{K}^{-1}\varphi_h\boldsymbol{u}_h\big)\cdot\boldsymbol{s}\ -\ \frac{d\varphi_D}{d\boldsymbol{s}}\right\|_{0,e}^2\ \leq\ C_5\,\|(\boldsymbol{u},\mathbf{p},\varphi)\ -\ (\boldsymbol{u}_h,\mathbf{p}_h,\varphi_h)\|^2\,.$$

Proof. For the derivation of the first two inequalities, it suffices to use Lemmas 6.1 and 6.2 in [8] or Lemmas 3.19 and 3.20 in [14]. Indeed, from there we have that for each piecewise polynomial ρ_h in $\mathcal{T}_h$, and for each $\rho\in\mathbf{L}^2(\Omega)$ with $\mathrm{rot}(\rho)=0$ in Ω, there exists $C>0$, independent of h, satisfying

$$h_T\|\mathrm{rot}(\rho_h)\|_{0,T}\leq C\,\|\rho-\rho_h\|_{0,T}\qquad\text{and}\quad h_e^{1/2}\|\,[\![\rho_h\,\boldsymbol{s}]\!]\|_{0,e}\leq C\,\|\rho-\rho_h\|_{0,\omega_e}\,. \tag{3.29}$$

Thus, taking $\rho_h\ :=\ \mathbb{K}^{-1}\,\mathbf{p}_h\ +\ \mathbb{K}^{-1}\,\varphi_h\,\boldsymbol{u}_h$ and $\rho\ :=\ \mathbb{K}^{-1}\,\mathbf{p}\ +\ \mathbb{K}^{-1}\,\varphi\,\boldsymbol{u}\ =\ \nabla\varphi_h$ in (3.29), adding on $T\in\mathcal{T}_h$ and on $e\in\mathcal{E}_h$, and by proceeding as in (3.25)-(3.26) we can easily obtain (3.27) and (3.28). In turn, these same arguments combined with Lemma 3.26 in [14] (which requires φ_D to be a piecewise polynomial in $\mathrm{H}^1(\Gamma)$) allows us to deduce the last inequality. We omit further details since the result can be deduced analogously to [10, Lemma 3.15]. □

We end this section by noticing that the efficiency property of the estimator $\boldsymbol{\theta}$ is a consequence of its own definition and Lemmas 3.9, 3.10 and 3.11.

4 A posteriori estimation: the 3d–case

In this section we briefly discuss how the a posteriori error analysis can be extended to the three dimensional case. To that end we first need to introduce some additional notations.

Given $\boldsymbol{\psi} = (\psi_1, \psi_2, \psi_3)$ a sufficiently smooth vector field, we let

$$\underline{\mathbf{curl}}(\boldsymbol{\psi}) := \nabla \times \boldsymbol{\psi} = \Big(\frac{\partial \psi_3}{\partial x_2} - \frac{\partial \psi_2}{\partial x_3}, \frac{\partial \psi_1}{\partial x_3} - \frac{\partial \psi_3}{\partial x_1}, \frac{\partial \psi_2}{\partial x_1} - \frac{\partial \psi_1}{\partial x_2} \Big),$$

and given any tensor field $\boldsymbol{\zeta} = (\zeta_{ij})_{1 \leq i,j \leq 3}$ we define

$$\mathbf{curl}\, \boldsymbol{\zeta} := \begin{pmatrix} \underline{\mathbf{curl}}(\zeta_{11}, \zeta_{12}, \zeta_{13}) \\ \underline{\mathbf{curl}}(\zeta_{21}, \zeta_{22}, \zeta_{23}) \\ \underline{\mathbf{curl}}(\zeta_{31}, \zeta_{32}, \zeta_{33}) \end{pmatrix} \quad \text{and} \quad \boldsymbol{\zeta} \times \boldsymbol{\nu} := \begin{pmatrix} (\zeta_{11}, \zeta_{12}, \zeta_{13}) \times \boldsymbol{\nu} \\ (\zeta_{21}, \zeta_{22}, \zeta_{23}) \times \boldsymbol{\nu} \\ (\zeta_{31}, \zeta_{32}, \zeta_{33}) \times \boldsymbol{\nu} \end{pmatrix},$$

Then, the local estimators $\boldsymbol{\theta}_{T,\mathtt{f}}$ and $\boldsymbol{\theta}_{T,\mathtt{h}}$ take the form

$$\begin{aligned} \boldsymbol{\theta}^2_{T,\mathtt{f}} &:= \|\mu\, \nabla \boldsymbol{u}_h - \boldsymbol{\sigma}_h^{\mathtt{d}} - (\boldsymbol{u}_h \otimes \boldsymbol{u}_h)^{\mathtt{d}}\|^2_{0,T} + \|\mathbf{div}(\boldsymbol{\sigma}_h) + \varphi_h\, \boldsymbol{g}\|^2_{0,T} \\ &\quad + h_T^2\, \|\mathbf{curl}\big((\boldsymbol{\sigma}_h + \boldsymbol{u}_h \otimes \boldsymbol{u}_h)^{\mathtt{d}}\big)\|^2_{0,T} + \sum_{e \in \mathcal{E}_{h,T}(\Omega)} h_e\, \|[\![(\boldsymbol{\sigma}_h + \boldsymbol{u}_h \otimes \boldsymbol{u}_h)^{\mathtt{d}} \times \boldsymbol{\nu}]\!]\|^2_{0,e} \\ &\quad + \sum_{e \in \mathcal{E}_{h,T}(\Gamma)} \|\boldsymbol{u}_h - \boldsymbol{u}_D\|^2_{0,e} + h_e \Big\| (\boldsymbol{\sigma}_h + \boldsymbol{u}_h \otimes \boldsymbol{u}_h)^{\mathtt{d}} \times \boldsymbol{\nu} - \mu \nabla \boldsymbol{u}_D \times \boldsymbol{\nu} \Big\|^2_{0,e}, \end{aligned}$$

$$\begin{aligned} \boldsymbol{\theta}^2_{T,\mathtt{h}} &:= \|\mathbb{K}^{-1}\mathbf{p}_h + \mathbb{K}^{-1}\varphi_h\, \boldsymbol{u}_h - \nabla \varphi_h\|^2_{0,T} + \|\mathrm{div}(\mathbf{p}_h)\|^2_{0,T} \\ &\quad + h_T^2\, \|\underline{\mathbf{curl}}\big(\mathbb{K}^{-1}\mathbf{p}_h + \mathbb{K}^{-1}\varphi_h\, \boldsymbol{u}_h\big)\|^2_{0,T} + \sum_{e \in \mathcal{E}_{h,T}(\Omega)} h_e\, \|[\![\big(\mathbb{K}^{-1}\mathbf{p}_h + \mathbb{K}^{-1}\varphi_h\, \boldsymbol{u}_h\big) \times \boldsymbol{\nu}]\!]\|^2_{0,e} \\ &\quad + \sum_{e \in \mathcal{E}_{h,T}(\Gamma)} \|\varphi_h - \varphi_D\|^2_{0,e} + h_e \Big\| \big(\mathbb{K}^{-1}\mathbf{p}_h + \mathbb{K}^{-1}\varphi_h\, \boldsymbol{u}_h\big) \times \boldsymbol{\nu} - \nabla \varphi_D \times \boldsymbol{\nu} \Big\|^2_{0,e}, \end{aligned}$$

and the global a posteriori error indicator is defined as

$$\boldsymbol{\theta} := \Big\{ \sum_{T \in \mathcal{T}_h} \boldsymbol{\theta}^2_{T,\mathtt{f}} + \sum_{T \in \mathcal{T}_h} \boldsymbol{\theta}^2_{T,\mathtt{h}} \Big\}^{1/2}.$$

The reliability of this estimator can be proved essentially by using the same arguments employed for the two dimensional case. In particular, analogously to the 2D case, here it is needed a stable Helmholtz decomposition for $\mathbf{H}(\mathrm{div}; \Omega)$. This result taken from [19, Theorem 3.1] is established next.

Lemma 4.1 *For each $\boldsymbol{v} \in \mathbf{H}(\mathrm{div}; \Omega)$ there exist $z \in \mathrm{H}^2(\Omega)$ and $\boldsymbol{\chi} \in \mathbf{H}^1(\Omega)$, such that there hold $\boldsymbol{v} = \nabla z + \underline{\mathbf{curl}}\, \boldsymbol{\chi}$ in Ω, and*

$$\|z\|_{2,\Omega} + \|\boldsymbol{\chi}\|_{1,\Omega} \leq C \|\boldsymbol{v}\|_{\mathrm{div};\Omega},$$

where C is a positive constant independent of $\boldsymbol{v}$.

Finally, to prove the efficiency of the three dimensional estimator it suffices to estimate the new terms since the analysis of the rest of the terms is straightforward. The following lemma provides these desired estimates, where, for the sake of simplicity, we assume that $\boldsymbol{u}_D$ and φ_D are piecewise polynomials. Otherwise, these data are replaced by suitable polynomial approximations of them, yielding high order terms in the error estimate (3.4).

Lemma 4.2 *There exist positive constants c_i, $i \in \{1,2,3\}$, independent of h, such that*

a) $$\sum_{T\in\mathcal{T}_h} h_T^2 \,\|\underline{\mathbf{curl}}\big(\mathbb{K}^{-1}\mathbf{p}_h + \mathbb{K}^{-1}\varphi_h\,\boldsymbol{u}_h\big)\|_{0,T}^2 \leq c_1\,\|(\boldsymbol{u},\mathbf{p},\varphi) - (\boldsymbol{u}_h,\mathbf{p}_h,\varphi_h)\|^2.$$

b) $$\sum_{e\in\mathcal{E}_{h,T}(\Omega)} h_e\,\|[\![\big(\mathbb{K}^{-1}\mathbf{p}_h + \mathbb{K}^{-1}\varphi_h\,\boldsymbol{u}_h\big)\times\boldsymbol{\nu}]\!]\|_{0,e}^2 \leq c_2\,\|(\boldsymbol{u},\mathbf{p},\varphi) - (\boldsymbol{u}_h,\mathbf{p}_h,\varphi_h)\|^2.$$

c) $$\sum_{e\in\mathcal{E}_{h,T}(\Gamma)} h_e\Big\|\big(\mathbb{K}^{-1}\mathbf{p}_h + \mathbb{K}^{-1}\varphi_h\,\boldsymbol{u}_h\big)\times\boldsymbol{\nu} - \nabla\varphi_D\times\boldsymbol{\nu}\Big\|_{0,e}^2 \leq c_2\,\|(\boldsymbol{u},\mathbf{p},\varphi) - (\boldsymbol{u}_h,\mathbf{p}_h,\varphi_h)\|^2.$$

Proof. By applying (3.25) and the fact that $\|\boldsymbol{u}_h\|_{1,\Omega}, \|\varphi\|_{1,\Omega} \leq r$, estimates a), b) and c) can be deduced from a slight modification of the proofs of [23, Lemma 4.9], [23, Lemma 4.10] and [23, Lemma 4.13], respectively. □

5 Numerical Results

Our objective here is to illustrate the properties of the a posteriori error estimator $\boldsymbol{\theta}$ (cf. (3.3)) studied in the previous sections via an associated adaptive algorithm. To this end, we report below a couple of examples implemented in the two–dimensional setting using the public domain finite element software *FreeFem++* which provides the automatic adaptation procedure tool `adaptmesh` [27].

As usual, the errors and the experimental convergence rates will be computed as

$$\mathtt{e}(\boldsymbol{\sigma}) := \|\boldsymbol{\sigma}-\boldsymbol{\sigma}_h\|_{\mathbf{div};\Omega}\,, \quad \mathtt{e}(\boldsymbol{u}) := \|\boldsymbol{u}-\boldsymbol{u}_h\|_{1,\Omega}\,,$$

$$\mathtt{e}(\mathbf{p}) := \|\mathbf{p}-\mathbf{p}_h\|_{\mathrm{div};\Omega}\,, \quad \mathtt{e}(\varphi) := \|\varphi-\varphi_h\|_{1,\Omega}$$

and

$$r(\boldsymbol{\sigma}) := \frac{-2\log(\mathtt{e}(\boldsymbol{\sigma})/\mathtt{e}'(\boldsymbol{\sigma}))}{\log(N/N')}\,, \quad r(\boldsymbol{u}) := \frac{-2\log(\mathtt{e}(\boldsymbol{u})/\mathtt{e}'(\boldsymbol{u}))}{\log(N/N')}$$

$$r(\mathbf{p}) := \frac{-2\log(\mathtt{e}(\mathbf{p})/\mathtt{e}'(\mathbf{p}))}{\log(N/N')}\,, \quad r(\varphi) := \frac{-2\log(\mathtt{e}(\varphi)/\mathtt{e}'(\varphi))}{\log(N/N')}\,,$$

where N and N' denote the total degrees of freedom associated to two consecutive triangulations with errors $\mathtt{e}(\cdot)$ and $\mathtt{e}'(\cdot)$. In turn, the total error, the total convergence rate and the effectivity index associated to the global estimator $\boldsymbol{\theta}$ are denoted and defined, respectively, as

$$\mathtt{e} = \big\{\,\mathtt{e}(\boldsymbol{\sigma})^2 + \mathtt{e}(\boldsymbol{u})^2 + \mathtt{e}(\mathbf{p})^2 + \mathtt{e}(\varphi)^2\,\big\}^{1/2}\,, \qquad \mathtt{r} = \frac{-2\log(\mathtt{e}/\mathtt{e}')}{\log(N/N')}\,, \quad \text{and} \quad \mathtt{eff}(\boldsymbol{\theta}) = \frac{\mathtt{e}}{\boldsymbol{\theta}}\,.$$

Test 1: accuracy assessment.

In this example we test the accuracy of our method as well as the reliability and the effectivity properties of the a posteriori error estimator $\boldsymbol{\theta}$ (3.3) via the the associated effectivity index $\mathtt{eff}(\boldsymbol{\theta})$ by using both quasi–uniform and adaptive refinement strategies. We consider on $\Omega = (-1,1)^2$ the smooth solution $(\boldsymbol{u}, p, \varphi)$ to problem (2.1) given by

$$\boldsymbol{u}(x_1,x_2) = \begin{pmatrix} 2\pi\cos(\pi x_2)\sin^2(\pi x_1)\sin(\pi x_2) \\ -2\pi\cos(\pi x_1)\sin(\pi x_1)\sin^2(\pi x_2) \end{pmatrix}, \quad p(x_1,x_2) = 5x_1\sin x_2 \quad \text{and} \quad \varphi(x_1,x_2) = e^{x_1+x_2}\,,$$

in terms of which we properly define the corresponding right–hand side functions and the Dirichlet data φ_D and $\boldsymbol{u}_D$. We take here the gravitational force $\mathbf{g} = (0,-1)^t$, the kinematic viscosity $\mu = 0.5$ and the thermal conductivity tensor $\mathbb{K} = e^{x_1+x_2}\mathbb{I}$, which yields $\kappa_0 = e^{-2}$ and $\|\mathbb{K}^{-1}\|_{\infty,\Omega} = e^2$. In turn, the stabilization parameters are optimally chosen as in [11], that is,

$$\begin{aligned} \kappa_1 \,=\, \mu = 0.5 \quad \kappa_2 \,=\, 1\,, \quad \kappa_3 = \mu^2/2 = 0.125, \\ \kappa_4 \,=\, \frac{\kappa_0}{\|\mathbb{K}^{-1}\|^2_{\infty,\Omega}} \,=\, e^{-6}\,, \quad \kappa_5 \,=\, \frac{\kappa_0}{2} \,=\, \frac{1}{2}e^{-2}\,, \quad \kappa_6 \,=\, \frac{\kappa_0}{2\|\mathbb{K}^{-1}\|_{\infty,\Omega}} \,=\, \frac{1}{2}e^{-4}. \end{aligned} \tag{5.1}$$

In Table 1 we present the convergence history for the fully-mixed approximation using the two lowest order methods ($k = 0, 1$) of the Boussinesq problem both under quasi-uniform and adaptive refinement. As expected, it is observed in each case that the individual and the total convergence rates are optimal, and that the corresponding effectivity index remains always bounded.

Test 2: a vortex in a unit box.

In our second example we consider a known solution problem on the unit square $\Omega := (0,1)\times(0,1)$ [15, 29], in which the velocity $\boldsymbol{u} = (\boldsymbol{u}_1, \boldsymbol{u}_2)$, the pressure p and the temperature φ solution to (2.1) are given, respectively, by

$$\begin{aligned} \boldsymbol{u}_1(x_1,x_2) \,&=\, \Big[\Big(1 \,-\, \cos\Big(\frac{2\pi(e^{r_1x_1}-1)}{e^{r_1}-1}\Big)\Big)\,\sin\Big(\frac{2\pi(e^{r_2x_2}-1)}{e^{r_2}-1}\Big)\Big]\,\frac{r_2}{2\pi}\,\frac{e^{r_2x_2}}{e^{r_2}-1}\,, \\ \boldsymbol{u}_2(x_1,x_2) \,&=\, \Big[\,-\,\Big(1 \,-\, \cos\Big(\frac{2\pi(e^{r_2x_2}-1)}{e^{r_2}-1}\Big)\Big)\,\sin\Big(\frac{2\pi(e^{r_1x_1}-1)}{e^{r_1}-1}\Big)\Big]\,\frac{r_1}{2\pi}\,\frac{e^{r_1x_1}}{e^{r_1}-1}\,, \\ p(x_1,x_2) \,&=\, r_1\,r_2\,\sin\Big(\frac{2\pi(e^{r_1x_1}-1)}{e^{r_1}-1}\Big)\,\sin\Big(\frac{2\pi(e^{r_2x_2}-1)}{e^{r_2}-1}\Big)\,\frac{e^{r_1x_1+r_2x_2}}{(e^{r_1}-1)(e^{r_2}-1)}\,, \end{aligned}$$

where r_1 and r_2 are positive parameters and

$$\varphi(x_1,x_2) \,=\, \boldsymbol{u}_1(x_1,x_2) + \boldsymbol{u}_2(x_1,x_2)\,.$$

Here, the velocity vector field $\boldsymbol{u}$ is similar to a counter clockwise vortex whose center $(\widehat{x}_1, \widehat{x}_2)$, depending on the choice of r_1 and r_2, has the coordinates

$$\widehat{x}_1 \,=\, \frac{1}{r_1}\,\log\Big(\frac{e^{r_1}+1}{2}\Big)\,, \quad \text{and} \qquad \widehat{x}_2 \,=\, \frac{1}{r_2}\,\log\Big(\frac{e^{r_2}+1}{2}\Big)\,.$$

We have particularly taken $r_1 = r_2 = 4.5$, case in which $\widehat{x}_1 = \widehat{x}_2 \approx 0.829$, and so the vortex is located near the top–right corner of the domain. Again, the corresponding source terms in the Boussinesq model are defined so that the corresponding exact solution is given by $(\boldsymbol{u}, p, \varphi)$, the physical coeficients are taken as $\mu = 0.5$, $\mathbb{K} = \mathbb{I}$ and $\mathbf{g} = (0,-1)^t$, and thus, the parameters κ_1, κ_2 and κ_3 are given as in (5.1) in the previous example. The remaining stabilization parameters take now the form

$$\kappa_4 \,=\, \frac{\kappa_0}{\|\mathbb{K}^{-1}\|^2_{\infty,\Omega}} \,=\, 1\,, \quad \kappa_5 \,=\, \frac{\kappa_0}{2} \,=\, 0.5\,, \quad \kappa_6 \,=\, \frac{\kappa_0}{2\|\mathbb{K}^{-1}\|_{\infty,\Omega}} \,=\, 0.5. \tag{5.2}$$

In Table 2, we present the numerical results we have obtained by quasi-uniform refinements and adaptive procedures, both for the finite element families $\mathbb{RT}_0 - \mathbf{P}_1 - \mathbf{RT}_0 - \mathrm{P}_1$ ($k = 0$) and $\mathbb{RT}_1 - \mathbf{P}_2 - \mathbb{RT}_2 - \mathrm{P}_1$ ($k = 1$). In each case, it is observed that the effective indexes $\mathtt{eff}(\boldsymbol{\theta})$ remain bounded

N	$e(\boldsymbol{\sigma})$	$r(\boldsymbol{\sigma})$	$e(\boldsymbol{u})$	$r(\boldsymbol{u})$	$e(\mathbf{p})$	$r(\mathbf{p})$	$e(\varphi)$	$r(\varphi)$	`e`	`r`	`eff`($\boldsymbol{\theta}$)
Fully–mixed $\mathbb{RT}_0 - \mathbf{P}_1 - \mathbf{RT}_0 - \mathrm{P}_1$ scheme with quasi-uniform refinement											
159	178.475	–	29.710	–	8.760	–	2.784	–	181.003	–	0.952
423	143.352	0.448	19.920	0.747	6.808	0.515	1.271	1.603	144.895	0.455	0.946
1251	82.591	1.017	12.388	0.876	3.380	1.292	0.475	1.816	83.584	1.015	0.901
4215	45.894	0.967	6.945	0.953	1.904	0.944	0.244	1.095	46.456	0.967	0.879
15795	23.356	1.023	3.583	1.002	1.002	0.973	0.120	1.073	23.650	1.022	0.864
61311	11.897	0.995	1.801	1.014	0.505	1.010	0.058	1.064	12.043	0.995	0.860
237701	6.020	1.005	0.908	1.011	0.250	0.037	0.031	0.936	6.093	1.006	0.851
Fully–mixed $\mathbb{RT}_0 - \mathbf{P}_1 - \mathbf{RT}_0 - \mathrm{P}_1$ scheme with adaptive refinement according to $\boldsymbol{\theta}$											
963	95.313	–	14.834	–	4.287	–	0.0609	–	96.557	–	0.918
2472	57.533	1. 071	8.706	1.130	2.521	1.127	0.365	1.086	58.244	1.072	0.892
3933	45.537	1.007	7.157	0.844	1.798	1.454	0.274	1.244	46.132	1.004	0.881
6636	34.326	1.080	5.405	1.073	1.474	0.760	0.204	1.116	34.781	1.080	0.867
18210	20.854	0.987	3.357	0.943	0.899	0.980	0.125	0.970	21.142	0.986	0.863
30993	15.874	1.026	2.552	1.031	0.664	1.140	0.088	1.329	16.091	1.027	0.860
52338	12.196	1.006	1.977	0.975	0.513	0.981	0.071	0.829	12.366	1.005	0.856
Fully–mixed $\mathbb{RT}_1 - \mathbf{P}_2 - \mathbf{RT}_1 - \mathrm{P}_2$ scheme with quasi-uniform refinement											
495	112.121	–	19.406	–	4.354	–	0.836	–	113.874	–	0.859
1383	50.490	1.553	9.047	1.486	2.215	1.315	0.403	1.421	51.344	1.551	0.726
4209	18.010	1.852	2.785	2.117	0.688	1.102	0.071	3.126	18.237	1.860	0.669
14439	5.628	1.887	0.819	1.987	0.225	1.813	0.011	2.969	5.692	1.889	0.669
54381	1.462	2.033	0.209	2.058	0.060	1.992	0.002	2.591	1.479	2.033	0.669
213411	0.372	2.003	0.055	1.953	0.015	2.035	0.000	2.493	0.376	2.002	0.669
829029	0.095	2.019	0.014	2.027	0.004	2.033	0.000	2.152	0.096	2.019	0.667
Fully–mixed $\mathbb{RT}_1 - \mathbf{P}_2 - \mathbf{RT}_1 - \mathrm{P}_2$ scheme with adaptive refinement according to $\boldsymbol{\theta}$											
3219	26.293	–	3.226	–	1.111	–	0.113	–	26.513	–	0.747
5199	15.451	2.218	2.358	1.307	0.516	3.202	0.038	4.549	15.639	2.202	0.683
9165	8.351	2.171	1.208	2.361	0.374	1.134	0.029	0.991	8.446	2.173	0.690
17301	4.716	1.799	0.707	1.687	0.161	2.659	0.009	3.735	4.771	1.795	0.674
35490	2.182	2.145	0.334	2.089	0.068	2.397	0.004	1.880	2.208	2.144	0.689
67074	1.164	1.974	0.193	1.726	0.037	1.944	0.002	2.111	1.181	1.968	0.677
131688	0.575	2.090	0.100	1.938	0.018	2.183	0.001	1.897	0.584	2.086	0.677

Table 1: Test 1: Convergence history and effectivity indexes for the fully-mixed approximation of the Boussinesq problem under quasi-uniform and adaptive refinement according to the indicator $\boldsymbol{\theta}$

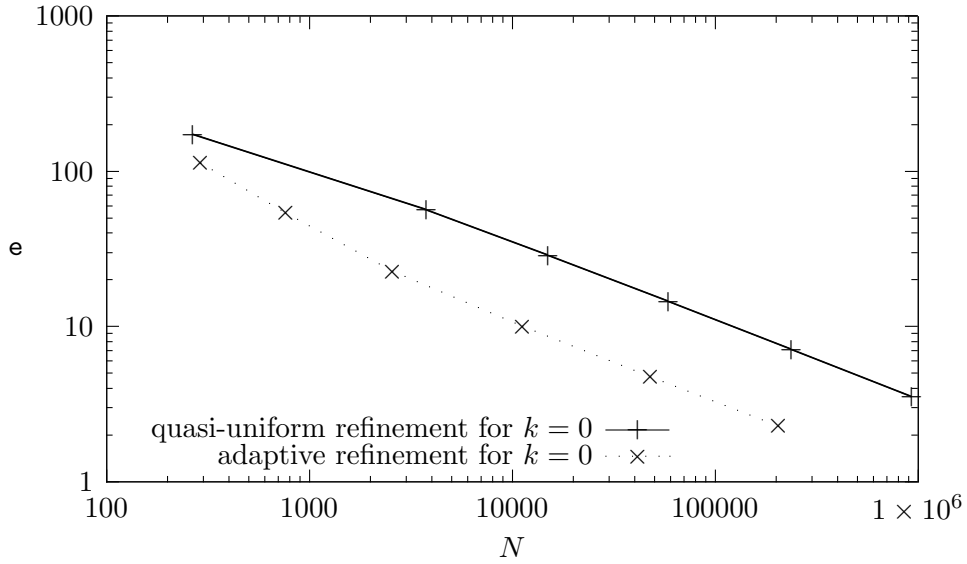

Figure 1: TEST 2: Decay of the total error with respect to the number of degrees of freedom using quasi-uniform and adaptive refinement strategies for $k = 0$.

and that the errors of the adaptive procedures decrease much faster than those obtained by the quasi–uniform ones. In fact, this reduction of the computational cost by adaptivity can be much better observed in Figures 1 and 2 where we plot the total error $\mathtt{e}$ versus the degrees of freedom N for both refinement strategies. In addition, Figure 3 shows how the refinement process is concentrated near the top–right corner of the domain because of the vortex there; this means that the algorithm induced by the a posteriori estimator $\boldsymbol{\theta}$ indeed properly guides the adaptive refinement process according to the quality of the total error approximation. We also present in Figure 3 some adapted meshes derived by the refinement process (first panel), and the post-processed pressure, the temperature vector field, the velocity magnitude and the post-processed vorticity along with the velocity vector field (second panel).

Test 3: adaptivity in a nonconvex domain

In this numerical experiment we set the problem in the nonconvex *pacman* domain

$$\Omega := \{ (x_1, x_2) \in \mathbb{R}^2 : \quad x_1^2 + x_2^2 \leq 1 \} \setminus (0,1)^2 ,$$

and the smooth solution $(\boldsymbol{u}, p, \varphi)$ where $\boldsymbol{u}$ is the same velocity vector field considered in the first test, the pressure is given by

$$p(x_1, x_2) = 5x_1 \operatorname{sin} x_2 + p_0 , \quad \text{where } p_0 \in \mathrm{R} \text{ is such that } \int_\Omega p = 0 ,$$

and the temperature is defined by

$$\varphi(x_1, x_2) = \frac{y}{(x_1 - a)^2 + (x_2 - b)^2} , \qquad \text{with} \quad a, b \in \mathbb{R}.$$

We here particularly take $a = b = 0.05$ so that the scalar field φ and the components of the vector variable $\mathbf{p}$ (depending on the temperature gradient) exhibit a singular behavior near the origin. In

N	$e(\boldsymbol{\sigma})$	$r(\boldsymbol{\sigma})$	$e(\boldsymbol{u})$	$r(\boldsymbol{u})$	$e(\mathbf{p})$	$r(\mathbf{p})$	$e(\varphi)$	$r(\varphi)$	`e`	`r`	$\texttt{eff}(\boldsymbol{\theta})$
Fully–mixed $\mathbb{RT}_0 - \mathbf{P}_1 - \mathbf{RT}_0 - \mathrm{P}_1$ scheme with quasi-uniform refinement											
267	117.421	–	6.314	–	125.925	–	7.732	–	172.466	–	0.999
1035	81.901	0.532	4.430	0.523	88.576	0.519	4.582	0.771	120.806	0.526	0.994
3771	39.806	1.116	1.900	1.309	39.993	1.230	2.003	1.281	56.494	1.176	0.987
14991	20.792	0.941	0.999	0.932	19.933	1.009	1.027	0.968	28.839	0.974	0.984
58995	10.510	0.996	0.533	0.917	10.034	1.002	0.543	0.930	14.551	0.999	0.982
236739	5.095	1.042	0.253	1.073	4.928	1.023	0.263	1.043	7.098	1.033	0.981
931359	2.560	1.005	0.128	0.995	2.434	1.030	0.130	1.029	3.537	1.017	0.981
Fully–mixed $\mathbb{RT}_0 - \mathbf{P}_1 - \mathbf{RT}_0 - \mathrm{P}_1$ scheme with adaptive refinement according to $\boldsymbol{\theta}$											
291	89.192	–	5.062	–	68.256	–	5.052	–	112.540	–	0.980
765	40.105	1.654	2.498	1.461	35.929	1.328	2.448	1.499	53.953	1.521	0.977
2580	16.642	1.447	0.909	1.663	15.235	1.411	0.889	1.666	22.598	1.432	0.979
11229	7.608	1.064	0.452	0.950	6.542	1.150	0.421	1.016	10.053	1.101	0.973
48111	3.557	1.045	0.218	1.002	3.134	1.012	0.208	0.969	4.750	1.031	0.971
205935	1.718	1.001	0.104	1.018	1.490	1.023	0.097	1.049	2.279	1.010	0.971
Fully–mixed $\mathbb{RT}_1 - \mathbf{P}_2 - \mathbf{RT}_1 - \mathrm{P}_2$ scheme with quasi-uniform refinement											
855	67.887	–	4.155	–	49.064	–	4.314	–	83.975	–	0.968
3429	23.739	1.513	1.757	1.239	22.842	1.101	2.064	1.059	33.055	1.343	0.959
13029	11.525	1.083	0.408	2.188	10.301	1.193	0.488	2.163	15.471	1.137	0.975
51297	2.951	1.988	0.087	2.255	2.841	1.880	0.098	2.349	4.098	1.939	0.967
203895	0.810	1.874	0.025	1.807	0.768	1.896	0.026	1.917	1.117	1.884	0.924
822159	0.192	2.065	0.006	2.064	0.184	2.050	0.006	2.067	0.266	2.058	0.926
Fully–mixed $\mathbb{RT}_1 - \mathbf{P}_2 - \mathbf{RT}_1 - \mathrm{P}_2$ scheme with adaptive refinement according to $\boldsymbol{\theta}$											
939	57.224	–	2.697	–	40.541	–	2.520	–	70.227	–	0.973
2427	15.427	2.761	0.395	4.046	13.671	2.289	0.364	4.075	20.620	2.581	0.984
8184	2.448	3.029	0.108	2.134	2.164	3.033	0.093	2.245	3.270	3.030	0.940
33336	0.555	2.113	0.026	2.028	0.479	2.147	0.021	2.119	0.734	2.128	0.943
128085	0.136	2.090	0.007	1.978	0.124	2.008	0.007	1.632	0.184	2.056	0.942

Table 2: Test 2: Convergence history and effectivity indexes for the fully-mixed approximation of the Boussinesq problem under quasi-uniform and adaptive refinement according to the indicator $\boldsymbol{\theta}$.

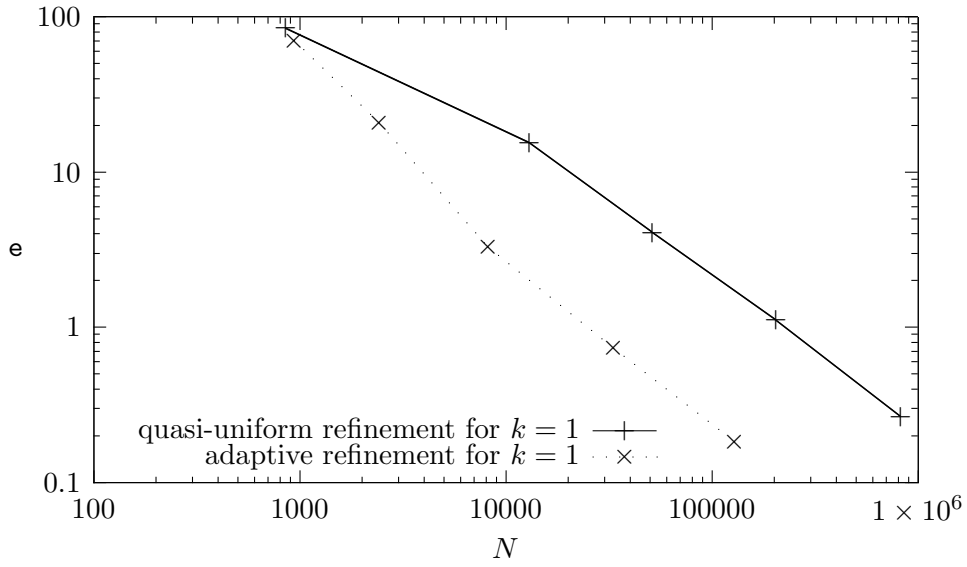

Figure 2: TEST 2: Decay of the total error with respect to the number of degrees of freedom using quasi-uniform and adaptive refinement strategies for $k = 1$.

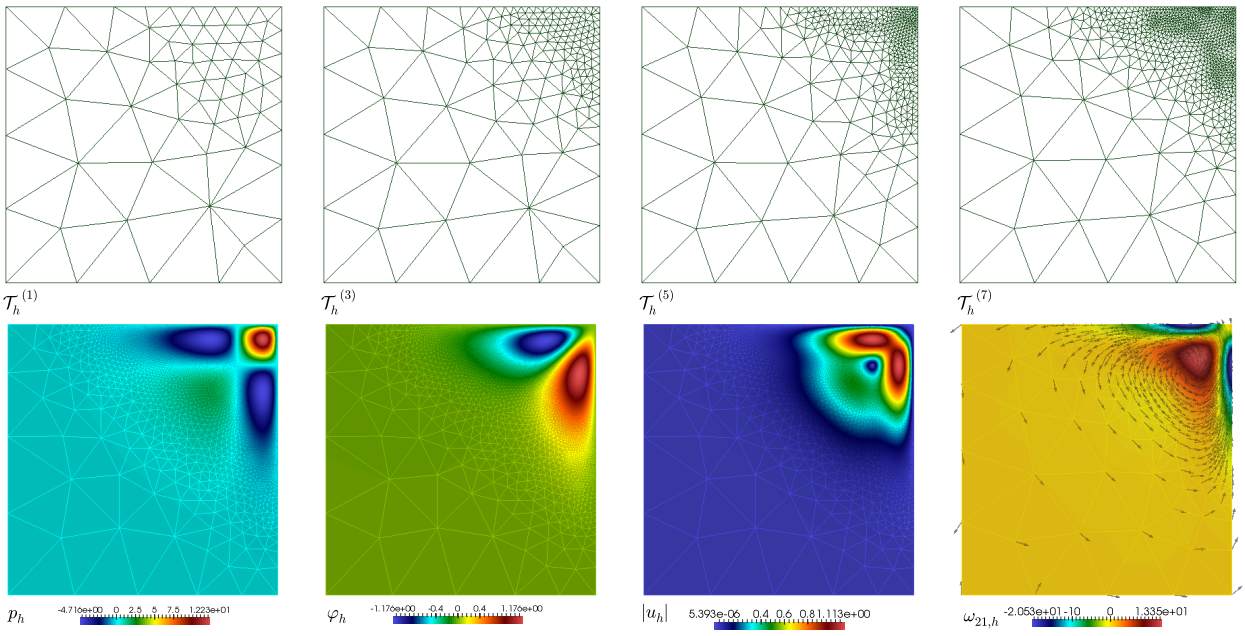

Figure 3: TEST 2: Snapshots of adapted meshes (first panel), post–processed pressure, temperature, velocity magnitude, and post-processed vorticity component $\omega_{21,h}$ along with the velocity field over the $7th$ adapted mesh (second panel) with $k = 0$, and $r_1 = r_2 = 4.5$.

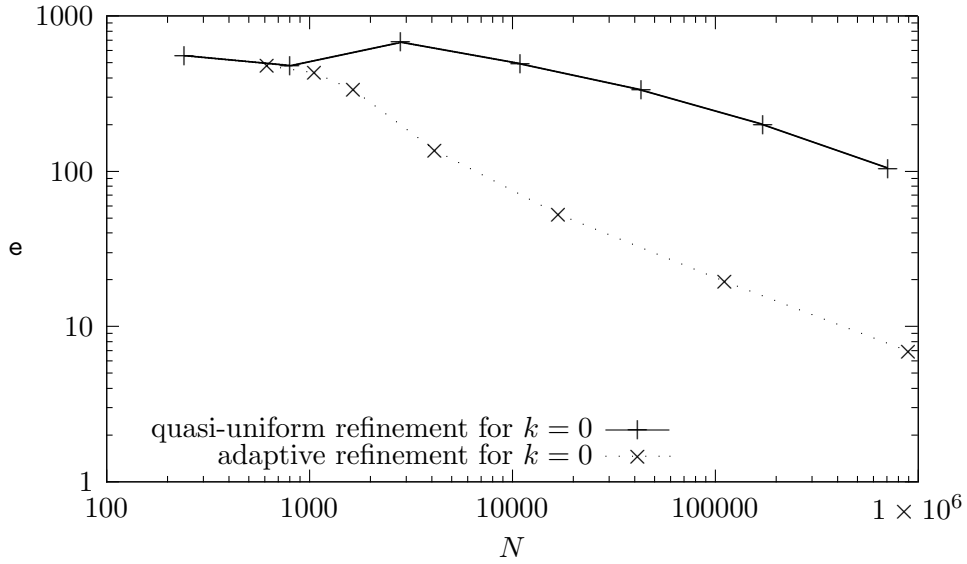

Figure 4: TEST 3: Decay of the total error with respect to the number of degrees of freedom using quasi-uniform and adaptive refinement strategies for $k = 0$.

turn, the physical coefficients are taken as $\mu = 0.5$, $\mathbb{K} = \mathbb{I}$ and $\mathbf{g} = (0, -1)^t$, and thus, the parameters κ_1, κ_2 and κ_3 are given as in (5.1) and κ_4, κ_5 and κ_6 by (5.2).

In Table 3, we summarize the convergence history associated to the augmented fully–mixed method for the Boussinesq problem using both quasi–uniform and adaptive refinement processes with the approximation orders $k = 0$ and $k = 1$. We observe that the individual convergence rates for the tensor $\boldsymbol{\sigma}$ and the velocity $\boldsymbol{u}$ are always quasi–optimal but, when using the quasi–uniform refinement strategy, the convergence of the approximation for vector $\mathbf{p}$ and the temperature field φ is oscillating, slower and/or lower than the expected one. This fact is even more evident for the case in which $k = 1$, where the total convergence rate is sub-optimal using quasi–uniform refinements; as expected due to the presence of the singularity. In turn, it can be observed that the adaptive algorithm not only restores the quasi–optimality in all the cases but also significantly reduces the computational cost. In fact, the latter statement can be better observed in Figures 4 and 5, where we contrast the total error decay with respect to the degrees of freedom using both refinement strategies for $k = 0$ and $k = 1$, respectively. In both cases, we clearly see that the total error decreases much faster with the adaptive algorithm, and with the expected convergence rates. Finally, in the first panel of Figure 6, we present some snapshots of adapted meshes obtained with the adaptive method and we observe there that the refinement process is concentrated in the origin, which is the zone with highest gradients. This illustrates that the a posteriori error estimator is indeed able to recognize the region in which the numerical approximation is deteriorated. In the second panel of Figure 6 we further present the velocity magnitude, the postprocessed pressure and the temperature vector fields obtained in some iterations using the adaptive method.

N	$e(\boldsymbol{\sigma})$	$r(\boldsymbol{\sigma})$	$e(\boldsymbol{u})$	$r(\boldsymbol{u})$	$e(\mathbf{p})$	$r(\mathbf{p})$	$e(\varphi)$	$r(\varphi)$	`e`	`r`	$\texttt{eff}(\boldsymbol{\theta})$
Fully–mixed $\mathbb{RT}_0 - \mathbf{P}_1 - \mathbf{RT}_0 - \mathrm{P}_1$ scheme with quasi-uniform refinement											
243	102.675	–	15.996	–	543.190	–	37.981	–	554.343	–	0.986
807	63.164	0.810	9.755	0.824	471.866	0.235	28.774	0.463	477.043	0.250	0.980
2823	33.516	1.012	5.2229	0.996	675.438	-0.573	27.200	0.090	676.836	-0.559	0.990
10959	17.032	0.998	2.612	1.023	490.267	0.472	18.597	0.561	490.922	0.474	0.989
43275	8.440	1.022	1.308	1.007	333.568	0.561	12.095	0.626	333.896	0.561	0.987
172647	4.222	1.001	0.657	0.995	199.337	0.744	6.819	0.828	199.499	0.744	0.986
708363	2.069	1.011	0.324	1.002	104.936	0.909	3.492	0.948	105.015	0.909	0.982
Fully–mixed $\mathbb{RT}_0 - \mathbf{P}_1 - \mathbf{RT}_0 - \mathrm{P}_1$ scheme with adaptive refinement according to $\boldsymbol{\theta}$											
618	70.158	–	10.644	–	472.867	–	28.836	–	479.030	–	0.982
1056	60.905	0.528	9.414	0.458	425.140	0.397	22.882	0.863	430.193	0.401	0.991
1653	56.541	0.332	8.740	0.332	328.488	1.151	11.967	2.893	333.648	1.134	0.986
4158	37.584	0.885	5.748	0.909	130.223	2.006	5.207	1.804	135.760	1.950	0.971
16812	19.770	0.920	3.155	0.859	48.568	1.412	2.271	1.188	52.582	1.358	0.945
111366	7.680	1.000	1.224	1.002	17.918	1.055	0.857	1.031	19.552	1.046	0.929
896418	2.692	1.005	0.429	1.005	6.336	0.997	0.301	1.003	6.904	0.998	0.888
Fully–mixed $\mathbb{RT}_1 - \mathbf{P}_2 - \mathbf{RT}_1 - \mathrm{P}_2$ scheme with quasi-uniform refinement											
771	43.271	–	5.593	–	350.846	–	23.452	–	354.326	–	0.883
2673	13.570	1.865	2.012	1.645	236.824	0.632	17.040	0.514	237.832	0.641	0.851
9585	4.058	1.891	0.566	1.986	402.511	-0.831	16.065	0.092	402.852	-0.825	0.969
37773	9.995	2.050	0.148	1.956	184.503	1.138	6.280	1.370	184.613	1.138	0.913
150303	0.247	2.018	0.036	2.047	83.432	1.149	2.632	1.259	83.474	1.149	0.940
601953	0.062	1.996	0.009	1.998	29.606	1.493	0.840	1.646	29.618	1.494	0.887
Fully–mixed $\mathbb{RT}_1 - \mathbf{P}_2 - \mathbf{RT}_1 - \mathrm{P}_2$ scheme with adaptive refinement according to $\boldsymbol{\theta}$											
2034	17.593	–	2.375	–	238.165	–	16.547	–	239.398	–	0.893
3288	14.285	0.867	1.930	0.864	220.719	0.317	11.457	1.531	221.486	0.324	0.975
5226	10.065	1.511	1.353	1.533	78.069	4.486	2.470	6.623	78.766	4.462	0.926
15618	3.618	1.869	0.513	1.772	14.219	3.111	0.564	2.698	14.692	3.068	0.920
70968	0.816	1.968	0.122	1.898	2.156	2.492	0.092	2.396	2.310	2.444	0.919
367374	0.155	2.020	0.024	1.978	0.399	2.052	0.017	2.054	0.429	2.048	0.922

Table 3: Test 3: Convergence history and effectivity indexes for the fully-mixed approximation of the Boussinesq problem under quasi-uniform and adaptive refinement according to the indicator $\boldsymbol{\theta}$ on the nonconvex *pacman* domain

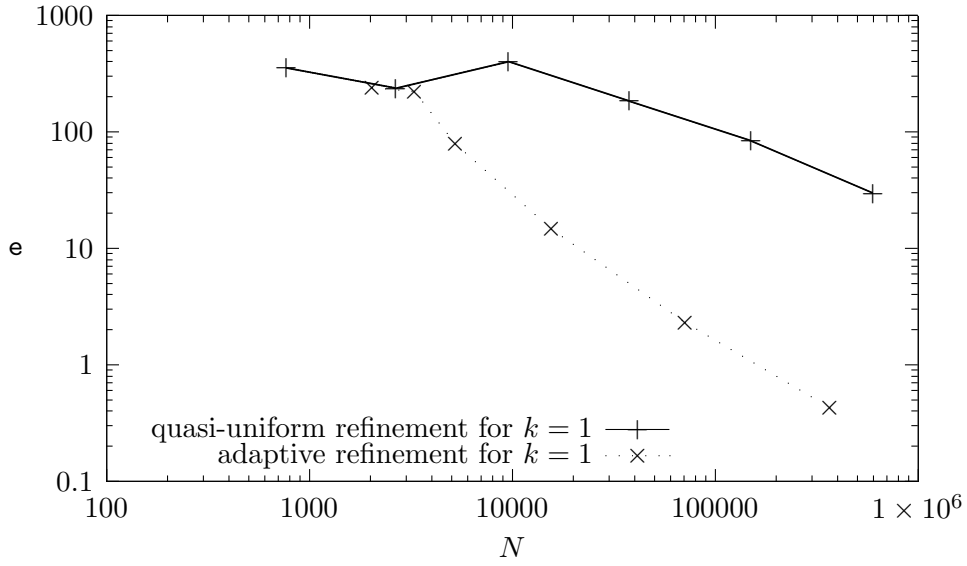

Figure 5: TEST 3: Decay of the total error with respect to the number of degrees of freedom using quasi-uniform and adaptive refinement strategies for $k = 1$.

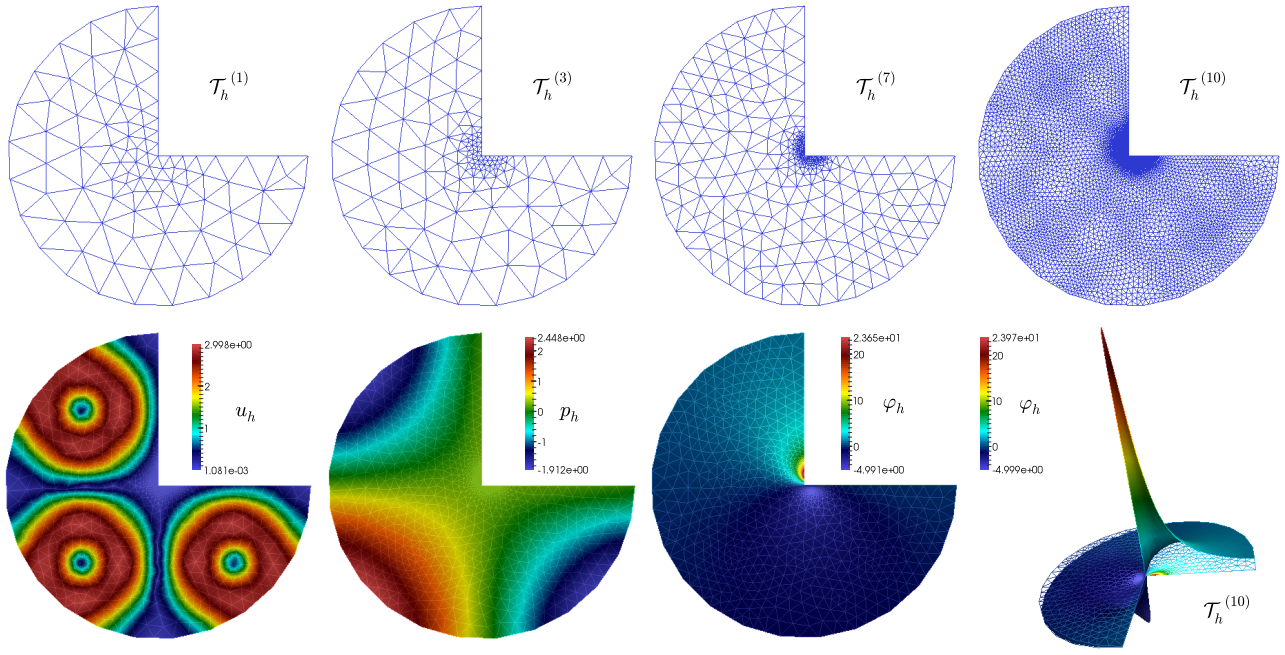

Figure 6: TEST 3: Snapshots of adapted meshes according to the indicator $\boldsymbol{\theta}$ (first row), velocity, post–processed pressure and temperature obtained in the $7th$ adaptive iteration (second row).

References

[1] M. Ainsworth, J.T. Oden, *A unified approach to a posteriori error estimation based on element residual methods.* Numer. Math. 65 (1993), 23–50.

[2] M. Ainsworth, J.T. Oden, *A posteriori error estimators for the Stokes and Oseen equations.* SIAM J. Numer. Anal. 34 (1997), no. 1, 228–245.

[3] K. Allali, *A priori and a posteriori error estimates for Boussinesq equations.* Int. J. Numer. Anal. Model. 2 (2005), no. 2, 179–196.

[4] A. Alonso, *Error estimators for a mixed method*, Numer. Math. 74 (1996), 385–395.

[5] M. Álvarez, G. N. Gatica and R. Ruíz–Baier, *A posteriori error analysis for a viscous flow–transport problem.* ESAIM Math. Model. Numer. Anal. 50 (2016), no. 6, 1789–1816.

[6] S. Berrone, *Adaptive discretization of stationary and incompressible Navier–Stokes equations by stabilized finite element methods.* Comput. Meth. Appl. Mech. Eng. 190 (2001), 4435–4455.

[7] F. Brezzi and M. Fortin, *Mixed and Hybrid Finite Element Methods.* Springer-Verlag, 1991.

[8] C. Carstensen, *A posteriori error estimate for the mixed finite element method.* Math. Comp. 66 (1997), no. 218, 465–476.

[9] P.G. Clément, *Approximations by finite element functions using local regularization.* RAIRO Modl. Math. Anal. Numér. 9 (1975), 77–84.

[10] E. Colmenares, G. N. Gatica and R. Oyarzúa, *A posteriori error analysis of an augmented mixed–primal formulation for the stationary Boussinesq model.* Calcolo, to appear.

[11] E. Colmenares, G. N. Gatica and R. Oyarzúa, *An augmented fully–mixed finite element method for the stationary Boussinesq problem.* Calcolo 54 (2017), no. 1, 167–205.

[12] E. Colmenares, G. N. Gatica and R. Oyarzúa, *Analysis of an augmented mixed–primal formulation for the stationary Boussinesq problem.* Numer. Methods Partial Differential Equations 32 (2016), no. 2, 445–478.

[13] E. Colmenares, G. N. Gatica and R. Oyarzúa, *Fixed point strategies for mixed variational formulations of the stationary Boussinesq problem.* C.R. Math. Acad. Sci. Paris 354 (2016), no. 1, 57–62.

[14] C. Dominguez, G. N. Gatica and S. Meddahi, *A posteriori error analysis of a fully–mixed finite element method for a two-dimensional fluid–solid interaction problem.* J. Comput. Math. 33 (2015), no. 6, 606–641.

[15] V.J. Ervin and L.N. Ntasin *A posteriori error estimation and adaptive computation of viscoelastic fluid flow.* Numer. Methods Partial Differential Equations 21 (2005), 297–322.

[16] M. Farhloul, S. Nicaise and L. Paquet *A mixed formulation of Boussinesq equations: analysis of nonsingular solutions.* Math. Comp. 69 (2000), no. 231, 965–986.

[17] M. Farhloul, S. Nicaise and L. Paquet, *A refined mixed finite element method for the Boussinesq equations in polygonal domains.* IMA J. Numer. Anal. 21 (2001), no. 2, 525–551.

[18] G.N. Gatica, *A Simple Introduction to the Mixed Finite Element Method: Theory and Applications*. Springer Briefs in Mathematics. Springer, Cham, 2014.

[19] G. N. Gatica, *A note on stable Helmholtz decompositions in 3D.* Preprint 2016-03, Centro de Investigacion en Ingenieria Matematica (CI^2MA), Universidad de Concepcion, Chile, (2016).

[20] G. N. Gatica, R. Ruiz-Baier and G. Tierra, *A posteriori error analysis of an augmented mixed method for the Navier–Stokes equations with nonlinear viscosity.* Comp. Math. Appl. 72 (2016), no. 9, 2289-2310.

[21] G. N. Gatica, G. Hsiao and S. Meddahi, *A residual–based a posteriori error estimator for a two-dimensional fluid-solid interaction problem.* Numer. Math. 114 (2009), no. 1, 63–106.

[22] G. N. Gatica, L. F. Gatica and A. Márquez, *Analysis of a pseudostress-based mixed finite element method for the Brinkman model of porous media flow.* Numer. Math. 126 (2014), no. 4, 635–677.

[23] G. N. Gatica, L. F. Gatica and F. A. Sequeira, *A priori and a posteriori error analyses of a pseudostress-based mixed formulation for linear elasticity.* Comp. Math. Appl. 71 (2016), no. 2, 585–614.

[24] G. N. Gatica, A. Márquez and M. A. Sánchez, *Analysis of a velocity–pressure–pseudostress formulation for the stationary Stokes equations.* Comput. Methods Appl. Mech. Engrg. 199 (2010), no. 17-20, 1064–1079.

[25] G. N. Gatica, A. Márquez and M. A. Sánchez, *A priori and a posteriori error analyses of a velocity–pseudostress formulation for a class of quasi–Newtonian Stokes flows.* Comput. Methods Appl. Mech. Engrg. 200 (2011), no. 17-20, 1619–1636.

[26] V. Girault and P.-A. Raviart, *Finite Element Approximation of the Navier–Stokes Equations.* Lecture Notes in Mathematics, 749. Springer-Verlag, Berlin-New York, (1979).

[27] F. Hecht, *New development in FreeFem++.* Journal of Numerical Mathematics 20 (2012), no. 3-4, 251–265.

[28] Roberts, J.E. and Thomas, J.M., *Mixed and Hybrid Methods.* In: Handbook of Numerical Analysis, P.G. Ciarlet and J.L. Lions (Eds.), vol. II, Finite Element Methods (Part 1), North-Holland, Amsterdam, 1991.

[29] Y. Zhang, Y. Hou, H. Zuo. *A posteriori error estimation and adaptive computation of conduction convection problems.* Appl. Math. Model. 35 (2011), 2336–2347.

Centro de Investigación en Ingeniería Matemática (CI^{2}MA)

PRE-PUBLICACIONES 2017

2017-06 Celso R. B. Cabral, Luis M. Castro, Christian E. Galarza, Víctor H. Lachos: *Robust quantile regression using a generalized class of skewed distributions*

2017-07 Raimund Bürger, Julio Careaga, Stefan Diehl: *A simulation model for settling tanks with varying cross-sectional area*

2017-08 Raimund Bürger, Sudarshan K. Kenettinkara, Ricardo Ruiz-Baier, Hector Torres: *Non-conforming/DG coupled schemes for multicomponent viscous flow in porous media with adsorption*

2017-09 Thomas Führer, Norbert Heuer, Michael Karkulik, Rodolfo Rodríguez: *Combining the DPG method with finite elements*

2017-10 Cinthya Rivas, Rodolfo Rodríguez, Manuel Solano: *A perfectly matched layer for finite-element calculations of diffraction by metallic surface-relief gratings*

2017-11 Raimund Bürger, Pep Mulet, Lihki Rubio, Mauricio Sepúlveda: *Linearly implicit IMEX schemes for the equilibrium dispersive model of chromatography*

2017-12 Veronica Anaya, Zoa De Wijn, David Mora, Ricardo Ruiz-Baier: *Mixed displacement-rotation-pressure formulations for elasticity*

2017-13 Veronica Anaya, David Mora, Carlos Reales, Ricardo Ruiz-Baier: *A vorticity-pressure finite element formulation for the Brinkman-Darcy coupled problem*

2017-14 Mario Álvarez, Gabriel N. Gatica, Ricardo Ruiz-Baier: *A posteriori error analysis of a fully-mixed formulation for the Brinkman-Darcy problem*

2017-15 Daniele Boffi, Lucia Gastaldi, Rodolfo Rodríguez, Ivana Sebestova: *A posteriori error estimates for Maxwell eigenvalue problem*

2017-16 Gabriel N. Gatica: *A note on weak* convergence and compactness and their connection to the existence of the inverse-adjoint*

2017-17 Eligio Colmenares, Gabriel N. Gatica, Ricardo Oyarzúa: *A posteriori error analysis of an augmented fully-mixed formulation for the stationary Boussinesq model*

Para obtener copias de las Pre-Publicaciones, escribir o llamar a: Director, Centro de Investigación en Ingeniería Matemática, Universidad de Concepción, Casilla 160-C, Concepción, Chile, Tel.: 41-2661324, o bien, visitar la página web del centro: `http://www.ci2ma.udec.cl`







Centro de Investigación en
Ingeniería Matemática (CI²MA)
Universidad de Concepción

Casilla 160-C, Concepción, Chile
Tel.: 56-41-2661324/2661554/2661316
http://www.ci2ma.udec.cl